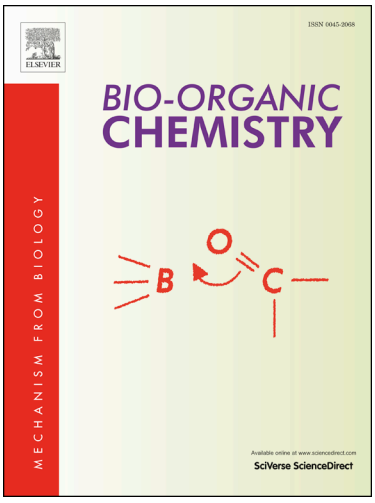

Design, synthesis and anticancer evaluation of 1*H*-pyrazolo[3,4-*d*]pyrimidine derivatives as potent EGFR^{WT} and EGFR^{T790M} inhibitors and apoptosis inducers

Ahmed A. Gaber, Ashraf H. Bayoumi, Ahmed M. El-morsy, Farag F. Sherbiny, Ahmed B.M. Mehany, Ibrahim H. Eissa

PII: S0045-2068(18)30301-8
DOI: https://doi.org/10.1016/j.bioorg.2018.06.017
Reference: YBIOO 2397

To appear in: *Bioorganic Chemistry*

Received Date: 28 March 2018
Revised Date: 7 June 2018
Accepted Date: 11 June 2018

Please cite this article as: A.A. Gaber, A.H. Bayoumi, A.M. El-morsy, F.F. Sherbiny, A.B.M. Mehany, I.H. Eissa, Design, synthesis and anticancer evaluation of 1*H*-pyrazolo[3,4-*d*]pyrimidine derivatives as potent EGFR^{WT} and EGFR^{T790M} inhibitors and apoptosis inducers, *Bioorganic Chemistry* (2018), doi: https://doi.org/10.1016/j.bioorg.2018.06.017

Design, synthesis and anticancer evaluation of 1*H*-pyrazolo[3,4-*d*]pyrimidine derivatives as potent EGFR^{WT} and EGFR^{T790M} inhibitors and apoptosis inducers

Ahmed A. Gaber[a], Ashraf H. Bayoumi[a], Ahmed M. El-morsy[a*], Farag F. Sherbiny[a], Ahmed. B. M. Mehany [b] Ibrahim H. Eissa[c]*

[a]Pharmaceutical organic chemistry department, Faculty of Pharmacy (Boys), Al-Azhar University, Cairo, 11884, Egypt

[b]Zoology department, Faculty of Science, Al-Azhar University, Cairo 11884, Egypt.

[c]Medicinal chemistry department, Faculty of Pharmacy (Boys), Al-Azhar University, Cairo, 11884, Egypt.

* **Corresponding authors:**

Ahmed M. El-morsy

Pharmaceutical organic chemistry department, Faculty of Pharmacy (Boys), Al-Azhar University, Nasr City 11884, Egypt

Email: Ahmedelmorsy232@yahoo.com

Ibrahim H. Eissa

Medicinal chemistry department, Faculty of Pharmacy (Boys), Al-Azhar University, Cairo, 11884, Egypt

Email: Ibrahimeissa@azhar.edu.eg

Abstract

In our attempt to develop effective EGFR-TKIs, two series of 1*H*-pyrazolo[3,4-*d*]pyrimidine derivatives were designed and synthesized. All the newly synthesized compounds were evaluated *in vitro* for their inhibitory activities against $EGFR^{WT}$. Compounds **15_b**, **15_j**, and **18_d** potently inhibited $EGFR^{WT}$ at sub-micro molar IC_{50} values comparable to that of erlotinib. Moreover, thirteen compounds that showed promising IC_{50} values against $EGFR^{WT}$ were tested *in vitro* for their inhibitory activities against mutant $EGFR^{T790M}$. Compounds **17_d** and **17_f** exhibited potent inhibitory activities towards $EGFR^{T790M}$ comparable to osimertinib. Compounds that showed promising IC_{50} values against $EGFR^{WT}$ were further tested for their anti-proliferative activities against three cancer cell lines bearing $EGFR^{WT}$ (MCF-7, HepG2, A549), and two cancer cell lines bearing $EGFR^{T790M}$ (H1975 and HCC827). Compounds **15_g, 15_j, 15_n, 18_d** and **18_e** were the most potent anticancer agents against the $EGFR^{WT}$ containing cells, while compounds**15_e**, **17_d** and **17_f** showed promising anti-proliferative activities against $EGFR^{T790M}$ containing cells. Furthermore, the most active compound **18_d** was selected for further studies regarding to its effects on cell cycle progression and induction of apoptosis in the HepG2 cell line. The results indicated that this compound is good apoptotic agent and arrests G_0/ $G_1$and G_2/M phases of cell cycle. Finally, molecular docking studies were performed to investigate binding pattern of the synthesized compounds with the prospective targets, $EGFR^{WT}$ (PDB: 4HJO) and $EGFR^{T790M}$ (PDB: 3W2O).

Key words: Anticancer; EGFR-TKIs; Docking; NSCLC; 1*H*-Pyrazolo[3,4-*d*]pyrimidine; $EGFR^{WT}$; $EGFR^{T790M}$

1. Introduction

Although there have been great advances in the detection and treatment of cancer, it remains one of the greatest medical challenges. Cancer is a huge global health burden, touching every region and socio-economic level. It is the second major cause of death worldwide, exceeded only by heart diseases [1]. When normal cells lose their regulatory mechanisms that control the growth and multiplication, cancer cells are produced. Cancer is caused by gene mutations or interfering with normal cell differentiation which initiated by drugs, viruses, smoking or diet [2].

It has been known that protein kinases (PKs) play a vital role in regulation of almost all major cellular functions, such as cell proliferation, growth, metabolism, survival, differentiation and apoptosis [3]. These enzymes catalyze the transfer of the gamma phosphate group from ATP to specific serine, threonine or tyrosine hydroxyl groups on target protein substrates involved in a number of cell signaling pathways [4]. The disruption of cell signaling cascades through kinase alterations (especially hyper-activation, hyper-production, or mutations) leads to several diseases, including cancer [5], inflammation [6], neurological disorders [7], autoimmune, cardiovascular disorders [8] and diabetes [9].

Epidermal growth factor receptor (EGFR) is one of the protein kinases family. It is a key mediator having a crucial role in cell growth, proliferation, survival, and migration [10, 11]. Overexpression of EGFR-tyrosine kinase (EGFR-TK) is a common feature in many human solid tumors as [12]. breast cancer [3] and hepatocellular carcinoma (HCC) [13]. Therefore, EGFR-TK is considered as a rational target for the design of new anticancer agents [14-16].

The discovery and development of novel therapeutic anti-EGFR-TK drugs for treatment of malignancy are some of the most important goals in modern medicinal chemistry. First-generation EGFR-tyrosine kinase inhibitors (EGFR-TKIs), erlotinib **1** [17] and gefitinib **2** [18, 19], provide significant clinical benefits in cases of non-small-cell lung cancer (NSCLC). However, disease progression develops ultimately after 9-14 months of treatment in most patients who respond to therapy. In addition, resistance due to EGFR-TK mutations affects about 50% of NSCLC patients [20, 21]. Second generation EGFR-TKIs as afatinib **3**[22] and canertinib **4** [23] have been developed to

overcome EGFR-TK mutation-related resistance and used clinically in treatment of NSCLC patients with actively mutated EGFR-TK. Unfortunately, these agents showed a relatively low maximal-tolerated-dose (MTD) due to the nonselective inhibition against wild-type EGFR-TK ($EGFR^{WT}$) and/or other kinases, leading to poor clinical patient outcomes [24, 25]. Third-generation EGFR-TKIs, rociletinib **5** [26] and avitinib **6** [27] showed advantageous properties in terms of residence times and toxicity profiles. Both rociletinib and avitinib were designated to treat mutant NSCLC. Rociletinib in phase III clinical trials exhibited serious hyperglycemia problem in NSCLC patients [28] (**Fig. 1**).

1*H*-Pyrazolo[3,4-*d*]pyrimidine nucleus is an important pharmacophore, presented in a number of anticancer agents [29-31], including EGFR-TKIs [32]. In 1997, compound **7** was generated by Novartis co-workers, using a pharmacophore model for ATP-competitive inhibitors interacting with the active site of the EGFR-TK. This compound showed low nanomolar efficacy for inhibiting the targeted enzyme, EGFR-TK [33]. Compound **8** is another example of 1*H*-pyrazolo [3,4-d]pyrimidines with anti EGFR-TK activity, having IC_{50} value of 5 nM against the BT474C cell line [34] (**Fig. 1**).

For several years, our research group has designed and synthesized many new anticancer derivatives [35-39]. Based on our previous researches and attractiveness of tyrosine kinases as promising targets for the design of new cancer agents, it was decided to introduce new 1*H*-pyrazolo[3,4-*d*]pyrimidine derivatives having inhibitory activities against wild-type EGFR-TK ($EGFR^{WT)}$ and mutant EGFR-TK ($EGFR^{T790M}$). Besides, the most active members were examined for their anti-proliferative activities against a number of cancer cell lines in which these types of enzyme exist. Moreover, the most active compound $\mathbf{18_d}$ was investigated for its apoptosis induction potential in HepG2 cell line. Cell cycle assay was performed to determine the cell phase which may be arrested by 1*H*-pyrazolo[3,4-*d*]pyrimidine derivatives. Finally, a molecular docking of the tested compounds was carried out to investigate their binding patterns with the prospective target.

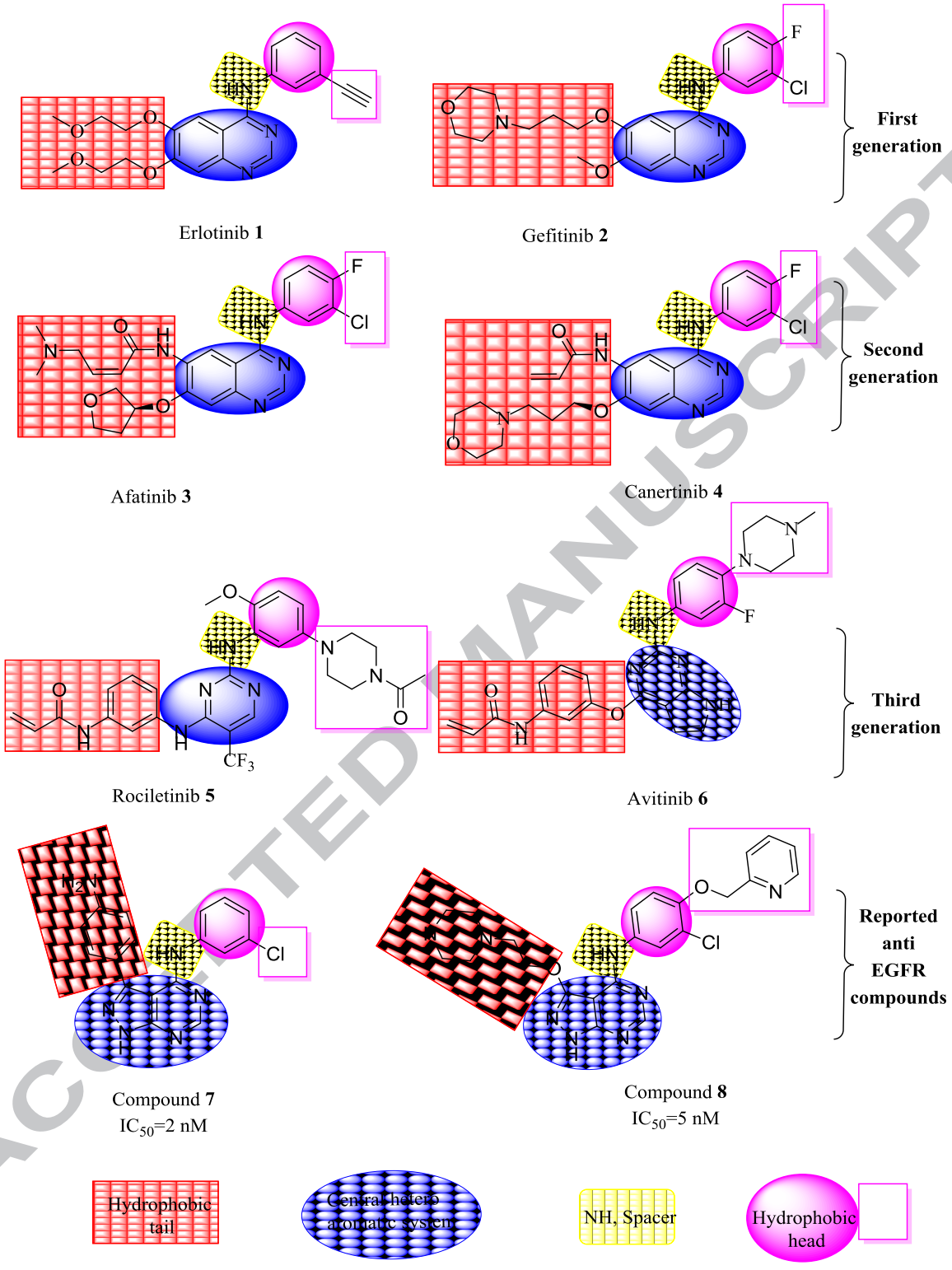

Fig. 1: Basic pharmacophoric features of EGFR-TK inhibitors.

1.1. Rational drug design

The ATP binding pocket of EGFR-TK consists of five main parts; adenine pocket, hydrophilic ribose pocket, hydrophobic region I, hydrophobic region II and phosphate binding region. (**Fig. 2**) [40-42]. The majority of EGFR-TKIs do not exploit the ribose and phosphate binding site [42]. Accordingly, structure-activity relationships (SAR) of EGFR-TKIs revealed that they have a Y shape [43] and share four common pharmacophoric features as shown in **Fig. 1** and **Fig. 3** [44].

i) The core structure of most inhibitors consists of a flat hetero aromatic ring system that contains at least one H-bond acceptor. It occupies the adenine binding pocket (hinge segment) and can form hydrogen bonding interactions with the key amino acid residues; Met793, Thr790 and Thr854 [45]. ii) Terminal hydrophobic head interacting with the hydrophobic region I. This hydrophobic head is a phenyl ring with different extra hydrophobic substitutions [44]. iii) Imino group (NH, spacer), occupying the linker region between the adenine binding region and the hydrophobic region I [46]. iv) Hydrophobic tail directly attached to the flat hetero aromatic ring system which occupies the hydrophobic region II [40, 47].

The main target of this work was synthesis of new 1*H*-pyrazolo[3,4-*d*]pyrimidines having the same essential pharmacophoric features of the reported and clinically used EGFR-TKIs as erlotinib **1** . The core of our molecular design rational comprised bioisosteric modification strategies of EGFR-TKIs at four different positions (**Fig. 4**).

The first position was the flat hetero aromatic ring system, where 1*H*-pyrazolo[3,4-*d*]pyrimidine nucleus was used as a bioisostere for quinazoline moiety of erlotinib **1** . The choice of this moiety was based on an important bio-isoeteric considerations. Frist of all, the bicyclic structure of 1*H*-pyrazolo[3,4-*d*]pyrimidine core is convenient to the large size space of the adenine binding region [43, 48]. Moreover, the heterocyclic nitrogen atoms serve as hydrogen-bond acceptors conferring excellent EGFR-TK potency [48]. The second position was the terminal hydrophobic head. Different hydrophobic moieties including (substituted) phenyl, aromatic heterocyclic, fused aromatic or aliphatic structures were selected. The third position was the linker (spacer) region, where the linker length as well as number of its hydrogen acceptor and/or hydrogen acceptor groups were modified. The different linkers may be one atom (e.g.

imino group as compound **19**), two atoms (e.g. hydrazono group as compound **16**), three atoms (e.g. ketohydrazinyl group as compounds **18**$_{a-e}$, methylenehydrazinyl group as compounds **15**$_{a-g,i,j}$ and acetohydrazonoyl group as compounds **15**$_{k-o}$), four atoms (e.g. thiosemicarbazide moiety as compounds **17**$_{a,c,e}$ and semicarbazide moiety as compounds **17**$_{b,d,f}$), five atoms (e.g. allylidenehydrazinyl moiety as compound **15**$_{h}$) or cyclic structure (e.g. pyrazole ring as compound **20**). The fourth position was the hydrophobic tail. Phenyl ring was incorporated at position-6 of 1*H*-pyrazolo[3,4-*d*]pyrimidine nucleus to occupy the hydrophobic region II of ATP binding site.

The wide variety of modifications enabled us to study the SAR of these compounds as effective anti-cancer agents with potential EGFR-TK inhibitory activity which is considered as a crucial objective of our work. All modification pathways and molecular design rationale were illustrated and summarized in **fig. 4** & **5**.

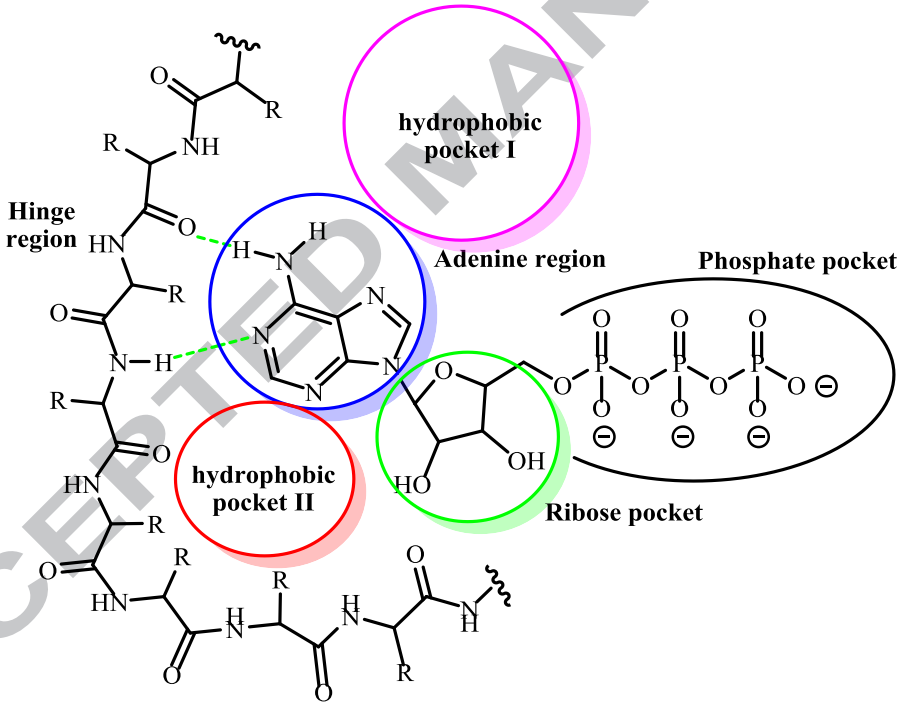

Fig. 2: ATP binding site of EGFR-TK cavity composed of five main parts [41].

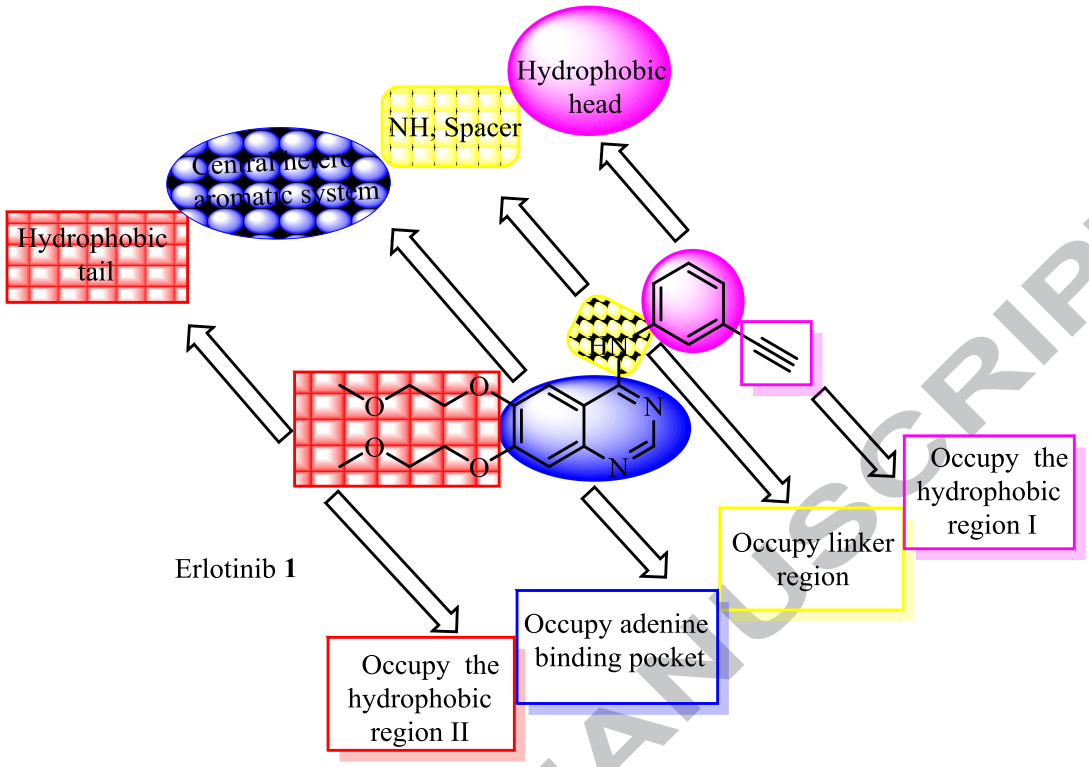

Fig. 3: The basic structural requirements for erlotinib as reported EGFR-TK inhibitor

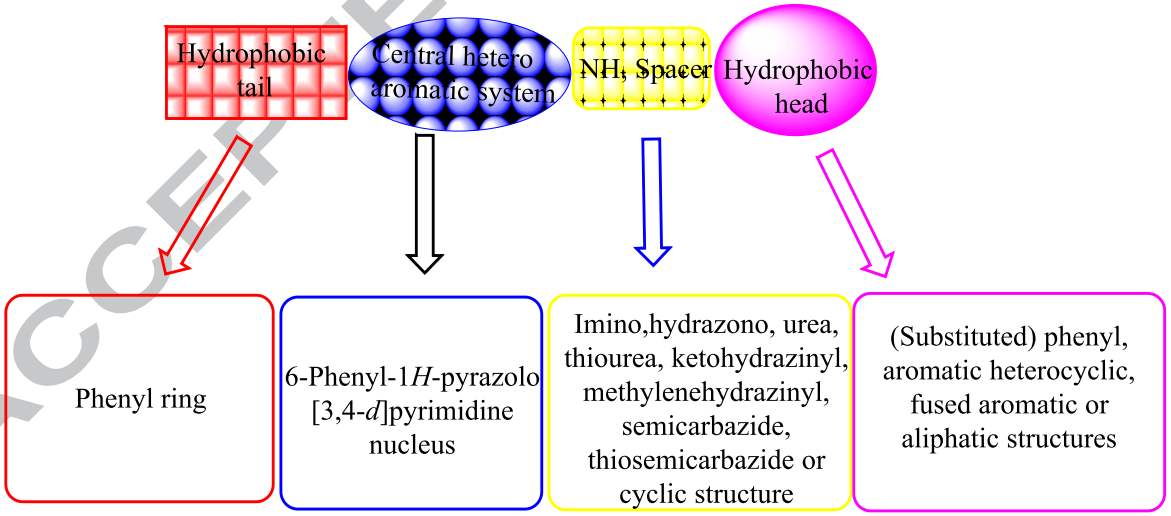

Fig. 4: Summary for the possible modifications of EGFR-TK inhibitors.

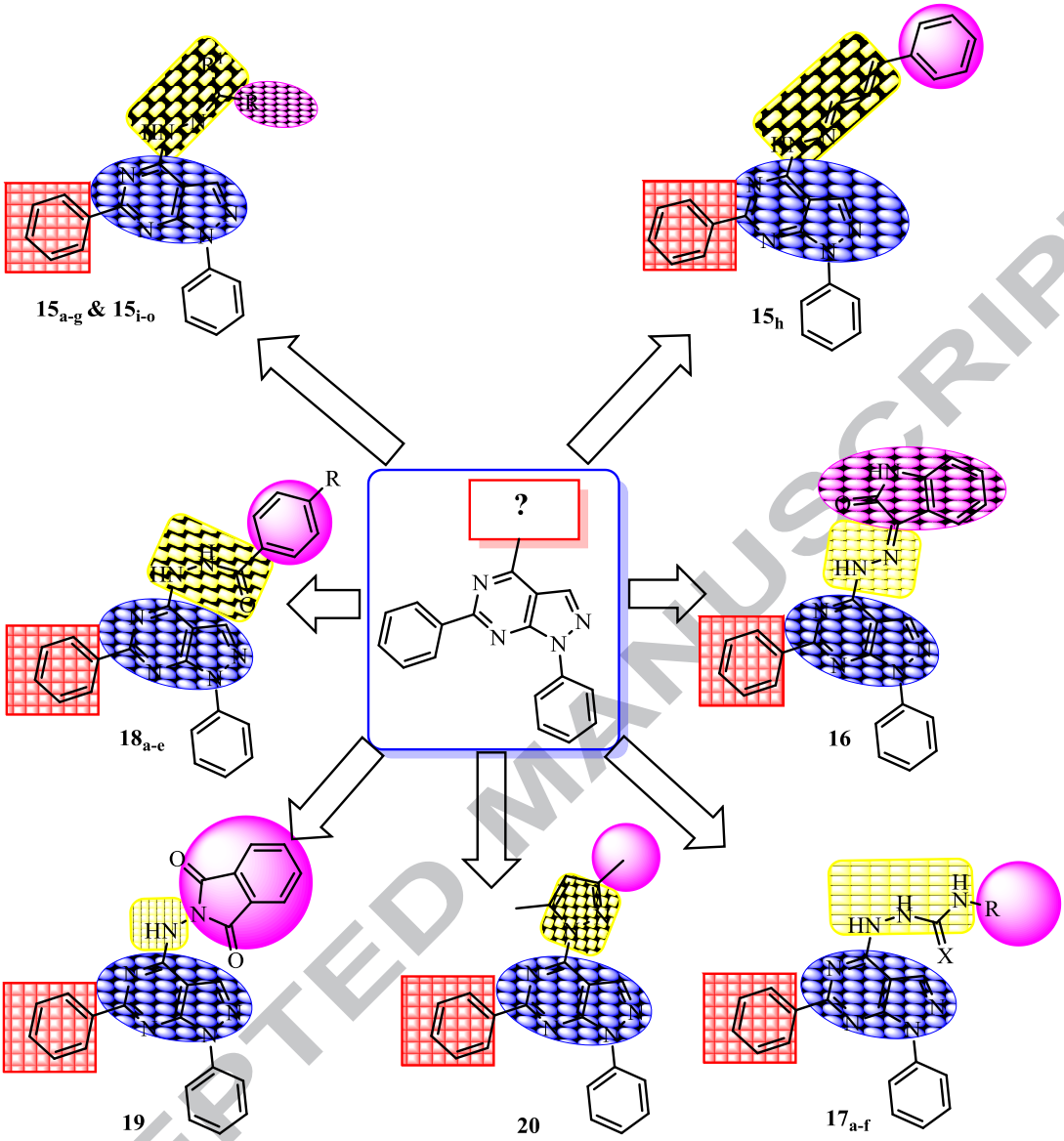

Fig. 5: Rational of molecular design of the new proposed EGFR-TK inhibitors

2. Results and discussion

2.1.Chemistry

The designed compounds were synthesized as outlined in **Schemes 1 & 2**. Ethoxymethylene malononitrile **9** [49] was allowed to react with phenyl hydrazine to produce 5-amino-1-phenyl-1*H*-pyrazole-4-carbonitrile **10** [29]. Compound **10** was underwent a partial hydrolysis using alcoholic NaOH to produce carboxamide derivative **11** [50]. 1,6-Diphenyl pyrazolo[3,4-*d*]pyrimidine core **12** [51] was formed from the

reaction of **11** with methyl benzoate with subsequent chlorination using phosphoryl trichloride to afford compound **13** [52]. The obtained compound **13** was heated with hydrazine hydrate to afford 4-hydrazinyl-1,6-diphenyl-1*H*-pyrazolo[3,4-*d*]pyrimidine **14**. The IR spectrum of **14** demonstrated stretching bands at 3444, 3352 and 3190 cm-^{1} corresponding to NH_2 and NH, respectively. Moreover, ^{1}H NMR of this compound showed two exchangeable signals at δ 4.73 and 9.89 ppm corresponding to NH_2 and NH, respectively. Refluxing of **14** with commercially available aromatic aldehydes or acetophenones in the presence of glacial acetic acid afforded the target compounds **15$_{a-o}$**. In addition, refluxing of **14** with commercially available isatin in the presence of glacial acetic acid afforded the target compound **16** (**Scheme 1**).

Reaction of compound **14** with appropriate isocyanates and/or isothiocyanates namely, ethyl isothiocyanates, ethyl isocyanates, cyclohexyl isothiocyanates, cyclohexyl isocyanates, phenyl isothiocyanates, and phenyl isocyanates, afforded the target thiosemicarbazide and semicarbazide derivatives **17$_{a-f}$**, respectively, depending on the reported procedure of thiosemicarbazide and semicarbazide syntheses [53-57]. ^{1}H NMR spectra of these compounds showed characteristic three D_2O exchangeable signals corresponding to three NH groups. The IR spectra of these compounds demonstrated stretching bands around 3320 cm^{-1} corresponding to the three NH groups, and other bands around 1666 cm^{-1} corresponding to C=O groups in compounds **17$_b$**, **17$_d$** and **17$_f$**. On the other hand, compound **14** was allowed to react with commercially available benzoyl chloride derivatives namely, benzoyl chloride, 4-methoxybenzoyl chloride, 4-methyl benzoyl chloride, 4-fluorobenzoyl chloride and 4-chlorobenzoyl chloride in presence of catalytic amount of TEA to produce the target benzohydrazide derivatives **18$_{a-e}$**, respectively. ^{1}H NMR spectra of compounds **18$_{a-e}$** exhibited two D_2O exchangeable signals corresponding to two NH groups. The IR spectra of these compounds demonstrated stretching bands ranging from 3320 to 3341 cm^{-1} corresponding to the two NH groups, and other bands ranging from 1672 to 1688 cm^{-1} corresponding to C=O groups Additionally, phthalimide derivative **19** was prepared by the reaction of compound **14** with commercially available phthalic anhydride, depending on the reported procedure [58]. The produced compound showed a characteristic D_2O exchangeable signal corresponding to the NH group. The IR spectrum of this compound demonstrated

stretching band at 3218 cm^{-1} corresponding to the NH group, and other band at 1713 cm^{-1} corresponding to the two C=O groups. Finally, treatment of compound **14** with acetylacetone yielded a pyrazolo derivative **20** (cyclized product). Compound **20** was characterized by ^1H NMR spectrum with absence of the D_2O exchangeable signal of NH proton. The IR spectrum of this compound demonstrated disappearance of stretching band of NH group due to the cyclization of the final compound (**Scheme 2**).

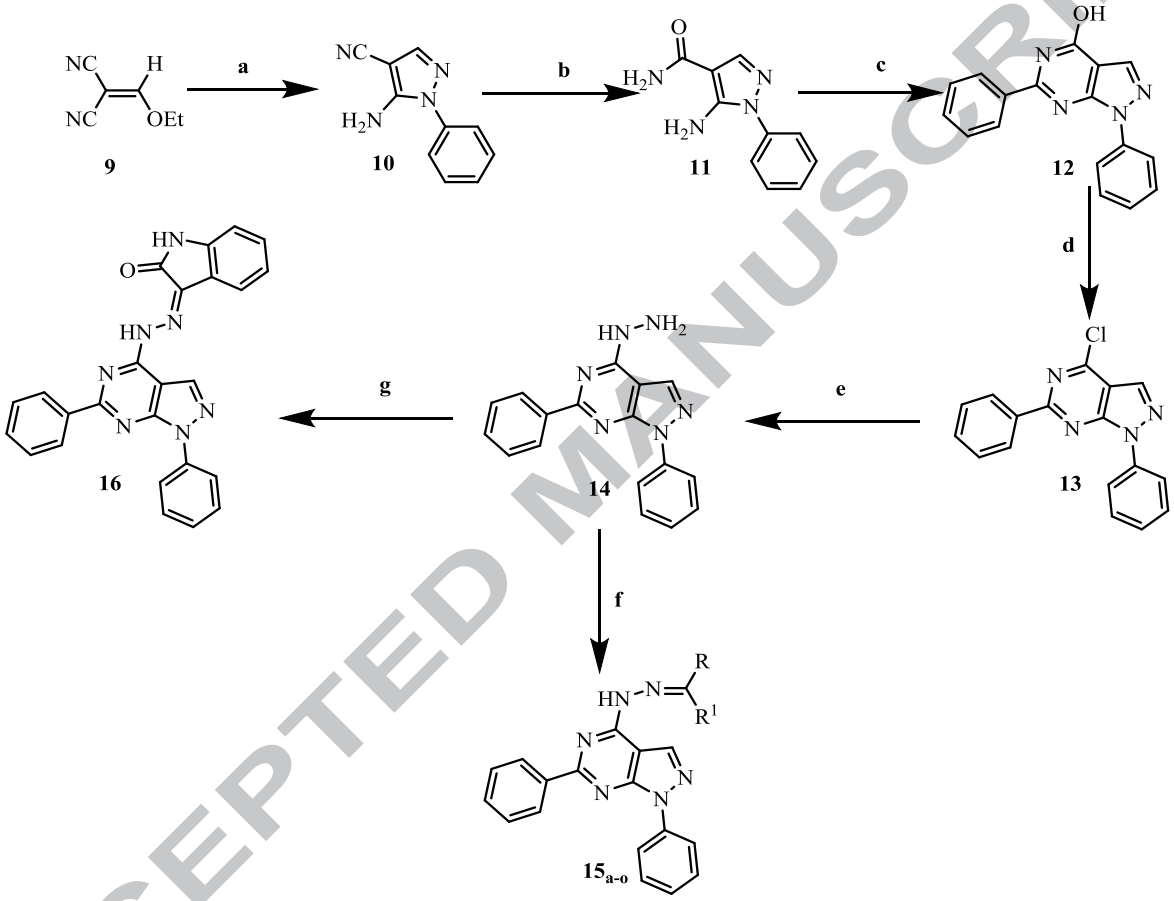

a) R = C_6H_5 R^1 = H **b)** R = 4-OHC_6H_4 R^1 = H
c) R = 4- $OCH_3C_6H_4$ R^1 = H **d)** R = 4- $CH_3C_6H_4$ R^1 = H
e) R = 4- $NO_2C_6H_4$ R^1 = H **f)** R = 4- ClC_6H_4 R^1 = H
g) R = 2,6-$Cl_2C_6H_3$ R^1 = H **h)** R = Cinnamyl R^1 = H
i) R = Thiophen-2-yl R^1 = H **j)** R = 1-Naphthayl R^1 = H
k) R = C_6H_5 $R^1 = CH_3$ **l)** R = 4- $NH_2C_6H_4$ $R^1 = CH_3$
m)R = 4- $CH_3C_6H_4$ $R^1 = CH_3$ **n)** R = 4- FC_6H_4 $R^1 = CH_3$
o) R = 4- BrC_6H_4 $R^1 = CH_3$

Scheme 1. Reagents and conditions of reaction; (a) phenyl hydrazine, absolute ethanol, reflux, 2 h; (b) sodium hydroxide, absolute ethanol, reflux, 5 h; (c) methyl benzoate,

sodium ethoxide, absolute ethanol, HCl, reflux, 14 h; (d) phosphoryl trichloride, reflux, 6 h; (e) hydrazine hydrate 99%, reflux, 8 h; (f) app. aromatic aldehydes or acetophenones, absolute ethanol, glacial acetic acid, reflux.; (g) isatin, glacial acetic acid, reflux, 24 h.

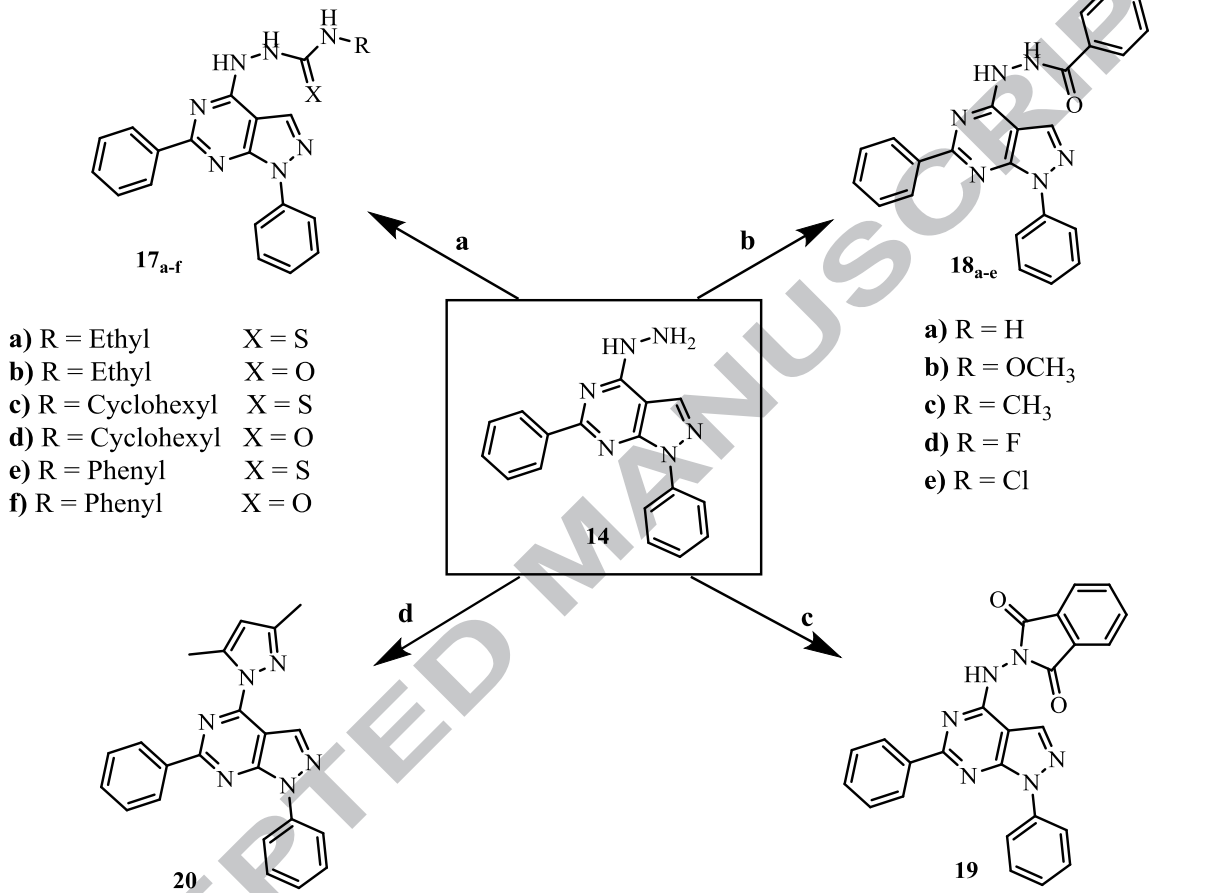

Scheme 2. Reagents and conditions of reaction: (a) app. isothiocyanates or isocyanates, butanol, RT; (b) app. benzoyl chlorides, DMF, RT.; (c) phthalic anhydride, glacial acetic acid, reflux 16 h; (d) acetyl acetone, glacial acetic acid, reflux 48 h.

2.2. Biological evaluation

2.2.1. EGFR^{WT} kinase inhibitory assay

According to the rational drug design, a series of novel EGFR^{WT} inhibitors bearing 1*H*-pyrazolo[3,4-*d*]pyrimidine scaffold were designed and synthesized. The kinase inhibitory activities of the synthesized compounds were evaluated according to Homogeneous time resolved fluorescence (HTRF) assay [59] against EGFR^{WT}. Erlotinib as one of the most potent EGFR^{WT} inhibitors was used as a positive control (**Table 1**).

In general, most of the synthesized compounds could interfere with the EGFR^{WT} activity exhibiting stronger activities than erlotinib as compounds **15_b, 15_e, 15_g, 15_h, 15_j, 15_n, 15_o, 17_a, 17_b, 17_d, 17_f, 18_d** and **18_e,** with IC_{50} values ranging from 0.09 ± 0.11 to 0.41 ± 0.21 µM. While compounds **15_c, 15_f, 15_i, 15_l, 17_c** and **17_e** showed comparable inhibitory activities to erlotinib with IC_{50} values ranging from 0.44 ± 0.24 to 0.73 ± 0.31 µM. . On the other hand, compounds **14, 15_a, 15_d, 15_k, 15_m, 16, 18_a, 18_b, 18_c** and **19** showed weaker activities than erlotinib with IC_{50} values ranging from 0.92 ± 0.43 to 4.91 ± 0.61 µM. Compound **20** was inactive against EGFR^{WT}**.**

The most active inhibitor was **18_d** (IC_{50} = 0.09 ± 0.11 µM), bearing a ketohydrazinyl linker between the phenyl group of the side chain and the 1*H*-pyrazolo[3,4-*d*]pyrimidine moiety. This compound was 4.5 times more active than erlotinib (IC_{50} = 0.42 ± 1.80 µM). However, replacing the chlorine atom with a fluorine one at the para position of phenyl moiety, the produced compound **18_e** showed a decreased inhibitory activity (IC_{50} = 0.41 ± 0.21 µM). Moreover, 4-methoxy and 4-methy substituted derivatives as compounds **18_b** (IC_{50} = 1.06± 0.28 µM), and **18_c** (IC_{50} = 1.54 ± 0.19 µM), respectively, showed lower activities than the 4-flouro and 4-chloro analogs indicating that grafting a large electron withdrawing substituents, as fluorine and chlorine, at the 4-positions is beneficial for the activity. With regard to the un-substituted derivative **18_a** (IC_{50} = 1.87± 0.32 µM), had a lower activity than the substituted ones.

When the ketohydrazinyl linker was replaced by a methylenehydrazinyl or acetohydrazonoyl ones, the yielded compounds **$15_{a-g,i,j}$** and **15_{k-o}** exhibited variable activities depending on the type of hydrophobic head. Compounds **15_b** (4-hydroxy phenyl derivative) and **15_j** (naphthyl derivative) were found to be the most potent counterparts in this two groups, as they were 2.2 and 2.6 times more active than erlotinib with IC_{50} values of 0.19 ± 0.13 and 0.16 ± 0.11 µM, respectively. Besides, compounds **15_e** (4-nitro phenyl derivative), **15_g** (2,6-dichloro phenyl derivative), **15_i** (thiophenyl derivative), **15_n** (4-flouro phenyl derivative) and **15_o** (4-bromo phenyl derivative), possessed excellent activities (IC_{50} = 0.23 ± 0.31, 0.28 ± 0.22, 0.51 ± 0.23, 0.34 ± 0.25 and 0.39 ± 0.17 µM, respectively). On the other hand, compounds **15_c** (4-methoxy phenyl derivative)**,** **15_f** (4-chloro phenyl derivative), and **15_l** (4-aminophenyl derivative)**,** showed almost equipotent activities with that of erlotinib with IC_{50} values of 0.49 ± 0.10, 0.44 ± 0.29 and 0.73 ± 0.31 µM, respectively. In addition, compounds **15_a** (phenyl derivative)**,** **15_d** (4-methyl phenyl derivative)**,** **15_k** (phenyl derivative) and **15_m** (4-methyl phenyl derivative), exhibited weaker anti $EGFR^{WT}$ activities with IC_{50} of 4.91 ± 0.61, 1.84 ± 0.19, 1.02 ± 0.41 and 0.92 ± 0.43 µM, respectively.

The addition of a long linker of four carbon atoms (thiosemicarbazide and semicarbazide moieties) between the hydrophobic head and the pyrazolo [3,4-*d*]pyrimidine moiety was beneficial. The majority of the produced compounds **17_a**, **17_b**, **17_d**, and **17_f** had inhibitory activities higher than that of erlotinib with IC_{50} values of 0.35 ± 0.21, 0.29 ± 0.14, 0.26 ± 0.14 and 0.32 ± 0.20 µM, respectively. While the other compounds **17_c** and **17_e** showed comparable inhibitory activities to erlotinib with IC_{50} values of 0.44 ± 0.24 and 0.56 ± 0.19 µM, respectively.

When linker extended to be five carbon atoms (allylidenehydrazinyl moiety), the yielded compound **15_h** exhibited strong activity with IC_{50} value of 0.32 ± 0.18 µM.

Finally, compound **20** incorporating a cyclic structure linker (pyrazole ring), was found to be inactive against $EGFR^{WT}$. The absence of suitable size of the hydrophobic head (e.g. phenyl ring) as a pharmacophoric feature in designing compound **20** may be the cause of its inactivity against $EGFR^{WT}$.

2.2.2. $EGFR^{T790M}$ kinase inhibitory assay

Thirteen compounds (**15_b**, **15_e**, **15_g**, **15_h**, **15_j**, **15_n**, **15_o**, **17_a**, **17_b**, **17_d**, **17_f**, **18_d** and **18_e)** that showed promising IC_{50} values against $EGFR^{WT}$ were further evaluated for their inhibitory activities against mutant $EGFR^{T790M}$. Osimertinib was tested as a positive control. The results revealed that compounds **17_d** (IC_{50} = 2.72 ± 0.21 nM) and **17_f** (IC_{50} = 3.90 ± 0.331nM) exhibited potent inhibitory activities towards $EGFR^{T790M}$ comparable to osimertinib (IC_{50} = 2.81 ± 1.6 nM). While compounds **15_j** and **18_d** possessed moderate activities with IC_{50} values of 4.81 ± 0.43 and 5.30 ± 0.52 nM, respectively. On the other hand, compounds **15_b**, **15_g**, **15_h**, **15_n**, **15_o**, **17_a**, **17_b** and **18_e** showed weak activities when compared with the reference drug, with IC_{50} values ranging from 6.54 ± 0.64 to 11.80 ± 1.13 nM (**Table 1**).

2.2.3. *In vitro* anti-proliferative activities

Thirteen compounds (**15_b**, **15_e**, **15_g**, **15_h**, **15_j**, **15_n**, **15_o**, **17_a**, **17_b**, **17_d**, **17_f**, **18_d** and **18_e)** that showed promising IC_{50} values against $EGFR^{WT}$ were further tested for their anti-proliferative activities against five cancer cell lines (human breast adenocarcinoma (MCF-7), hepatocellular carcinoma (HepG2) and non-small cell lung cancer cells (A549, H1975 and HCC827)) using on MTT assay [60]. MCF-7, HepG2 and A549 cells have the overexpressed $EGFR^{WT}$ [61-63], while H1975 and HCC827 cells harbor different EGFR mutations (H1975 harboring $EGFR^{L858R/T790M}$ mutation, and HCC827 harboring $EGFR^{del\ E746\text{-}A750}$ mutation) [64, 65]. Four commercially available drugs (lapatinib, sorafinib, erlotinib and osimertinib) were used in this test as positive controls.

As shown in **Table 2,** the obtained results revealed that most of the synthesized compounds showed excellent, moderate to weak anti-proliferative activities against the tested cell lines. For the activity against human breast adenocarcinoma cell line (MCF-7), compounds **15_b**, **15_e**, **15_g**, **15_h**, **15_j**, **15_n**, **18_d** and **18_e** were found to be more potent than lapatinib (IC_{50} = 6.60 ± 0.30 µM) with IC_{50} values ranging from 0.50 ± 1.90 to 4.90 ± 0.21 µM. While compounds **15_o**, **17_a**, **17_b**, **17_d** and **17_f**, were less potent than lapatinib with IC_{50} values ranging from 6.74 ± 1.92 to 12.07 ± 2.30 µM. For hepatocellular carcinoma cell line (HepG2), all the tested compounds were more potent than sorafenib (IC_{50} = 4.00 ± 0.4 µM) with IC_{50} values ranging from 0.01 ± 0.71 to 1.53 ± 0.72 µM.

For the activity against the wild-type non-small cell lung cancer cell line (A549), compounds **15_g**, **15_j**, **15_n**, **15_o**, **17_d**, **17_f**, **18_d** and **18_e** were more potent than erlotinib (IC_{50} = 1.80 ± 0.91 µM) with IC_{50} values ranging from 0.62 ± 1.70 to 1.70 **±** 0.21 µM. While compounds **15_b**, **15_e**, **15_h**, **17_a** and **17_b** were less potent than erlotinib with IC_{50} values ranging from 1.95 ± 1.01 to 4.16 ± 0.71 µM.

For the activity against the mutant-type non-small cell lung cancer cell line (H1975), compounds **15_e**, **17_d** and **17_f** were more potent than osimertinib (IC_{50} = 0.03 ± 0.08 µM) with IC_{50} values ranging from 0.02 ± 0.08 to 0.03 ± 0.07 µM. While compounds **15_b**, **15_j**, **15_n**, **17_b** and **18_d** showed moderate anti-proliferative activities with IC_{50} values ranging from 0.04 ± 0.01 to 0.06 ± 0.01µM. Moreover, compounds **15_g**, **15_h**, **15_o**, **17_a**, and **18_e** exhibited weak activities with IC_{50} values ranging from 0.07 ± 0.10 to 0.09 ± 0.27µM.

For the activity against the mutant-type non-small cell lung cancer cell line (HCC827), only compound **15_e** (IC_{50} = 0.04 ± 0.03 µM) was more potent than osimertinib (IC_{50} = 0.05 ± 0.01µM). While compounds **17_d** and **17_f** showed moderate anti-proliferative activities with IC_{50} values of 0.06 ± 0.24 and 0.09 ± 0.08 µM, respectively. Moreover, compounds **15_b**, **15_g**, **15_h**, **15_j**, **15_n**, **15_o**, **17_a**, **17_b**, **18_d** and **18_e** exhibited weak activities with IC_{50} values ranging from 0.11 ± 0.01 to 0.27 ± 0.49 µM.

Table 1: *In vitro* enzymatic inhibitory activities of the target of 1*H*-pyrazolo[3,4-*d*]pyrimidines against $EGFR^{WT}$ and $EGFR^{790M}$.

Comp.	$EGFR^{WT}$ IC_{50} (µM)[a]	$EGFR^{T790M}$ IC_{50} (nM)[a]	**Comp.**	$EGFR^{WT}$ IC_{50} (µM)[a]	$EGFR^{T790M}$ IC_{50} (nM)[a]
14	3.59 ± 0.30	NT[b]	**16**	3.85 ± 0.38	NT[b]
15_a	4.91 ± 0.61	NT[b]	**17_a**	**0.35 ± 0.21**	8.52 ± 0.80
15_b	**0.19 ± 0.13**	7.81 ± 0.71	**17_b**	**0.29 ± 0.14**	6.54 ± 0.64
15_c	0.49 ± 0.10	NT[b]	**17_c**	0.44 ± 0.24	NT[b]
15_d	1.84 ± 0.19	NT[b]	**17_d**	**0.26 ± 0.14**	**2.72 ± 0.21**
15_e	**0.23 ± 0.31**	3.20 ± 0.25	**17_e**	0.56 ± 0.19	NT[b]
15_f	0.44 ± 0.29	NT[b]	**17_f**	**0.32 ± 0.20**	3.90 ± 0.33

15_g	**0.28 ± 0.22**	10.32 ± 0.91	**18_a**	1.87 ± 0.32	NT[b]
15_h	**0.32 ± 0.18**	9.63 ± 0.90	**18_b**	1.06 ± 0.28	NT[b]
15_i	0.51 ± 0.23	NT[b]	**18_c**	1.54 ± 0.19	NT[b]
15_j	**0.16** ± 0.11	4.81 ± 0.43	**18_d**	**0.09 ± 0.11**	5.30 ± 0.52
15_k	1.02 ± 0.41	NT[b]	**18_e**	**0.41 ± 0.21**	8.41 ± 0.80
15_l	0.73 ± 0.31	NT[b]	**19**	2.78 ± 0.31	NT[b]
15_m	0.92 ± 0.43	NT[b]	**20**	NA[c]	NT[b]
15_n	**0.34 ± 0.25**	6.80 ± 0.62	**Erlotinib**	0.42 ± 1.80	NT[b]
15_o	**0.39 ± 0.17**	11.80 ± 1.13	**Osimertinib**	NT[b]	2.81 ± 1.6

[a] Data were expressed as Mean ± Standard error (S.E.) of three independent experiments.

[b] NT: Compounds not tested.

[c] NA: Compounds having IC_{50} value >50 µM.

[d] Bold figures indicate superior potency than erlotinib

Table 2: *In vitro* anti-proliferative activities towards MCF7, A549, HepG2, H1975 and HCC827 cell lines

Comp.	IC_{50} (µM)[a]				
	MCF7	HepG2	A549	H1975	HCC827
15_b	**2.36 ± 1.80**	**0.35 ± 1.61**	1.95 ± 1.01	0.06 ± 0.01	0.18 ± 0.01
15_e	**3.90 ± 0.80**	**0.04 ± 1.01**	2.90 ± 1.61	**0.03 ± 0.02**	**0.04 ± 0.03**
15_g	**1.89 ± 1.71**	**0.06 ± 1.71**	**1.07 ± 1.70**	0.08 ± 0.09	0.23 ± 0.09
15_h	**4.65 ± 0.30**	**0.44 ± 1.00**	4.16 ± 0.71	0.08 ± 0.03	0.22 ± 0.02
15_j	**0.81 ± 1.00**	**0.03 ± 0.21**	**1.70 ± 0.21**	0.04 ± 0.01	0.11 ± 0.01
15_n	**4.90 ± 0.21**	**0.27 ± 0.30**	**0.81 ± 1.01**	0.05 ± 0.47	0.15 ± 0.10
15_o	6.74 ± 1.92	**0.74 ± 1.62**	**1.22 ± 0.40**	0.09 ± 0.27	0.27 ± 0.49
17_a	12.07 ± 2.30	**1.53 ± 0.72**	2.64 ± 0.40	0.07 ± 0.10	0.19 ± 0.13
17_b	11.57 ± 2.51	**1.12 ± 1.71**	3.34 ± 1.61	0.05 ± 0.13	0.15 ± 0.08

17_d	9.10 ± 1.22	**0.04 ± 1.01**	**1.10 ± 0.21**	**0.02 ± 0.08**	0.06 ± 0.24
17_f	7.72 ± 1.21	**0.36 ± 0.33**	**0.96 ± 1.01**	**0.03 ± 0.07**	0.09 ± 0.08
18_d	**0.50 ± 1.90**	**0.01 ± 0.71**	**0.62 ± 1.70**	0.04 ± 0.33	0.12 ± 0.07
18_e	**1.61 ± 0.40**	**1.81 ± 1.04**	**0.85 ± 0.21**	0.07 ± 0.04	0.19 ± 0.05
Lapatinib	6.60 ± 0.30	NT[b]	NT[b]	NT[b]	NT[b]
Sorafenib	NT[b]	4.00 ± 0.42	NT[b]	NT[b]	NT[b]
Erlotinib	NT[b]	NT[b]	1.80 ± 0.91	NT[b]	NT[b]
Osimertinib	NT[b]	NT[b]	NT[b]	0.03 ± 0.08	0.05 ± 0.01

[a] IC_{50} values are the mean ± S.D. of three separate experiments.

[b] NT: Compounds not tested for their anti-proliferative activities.

[c] Bold figures indicate superior potency than positive controls.

2.2.4. *In-vitro* DNA-flow cytometric (cell cycle) analysis.

The most active compound **18_d** was selected for further studies regarding to its effect on cell cycle progression and induction of apoptosis in the HepG2 cell line. DMSO was used as a negative control. Cell cycle stages were being recognized through flow cytometry after PI staining followed by RNAse treatment. The HepG2 cells were incubated with 1 µM of this compound for 24 h, then its effect on the cell cycle profile was analyzed.

The results revealed that exposure of HepG2 cells to compound **18_d** leaded to an interference with the normal cell cycle distribution of this cell line. This compound induced a significant increase in the percentage of cells at phases of pre-G_1, which could be indicative of apoptosis, G_0/G_1 and G_2/M by 12, 1.7 and 1.2 folds respectively, comparing to the control. Such increase was accompanied by a significant decrease in the percentage of cells at the S-phase of the cell cycle. These result clearly indicated that compound **18_d** arrests G_0/ $G_1$and G_2/M phases of cell cycle **(Fig. 6. & Fig. 7 & Table 3)**.

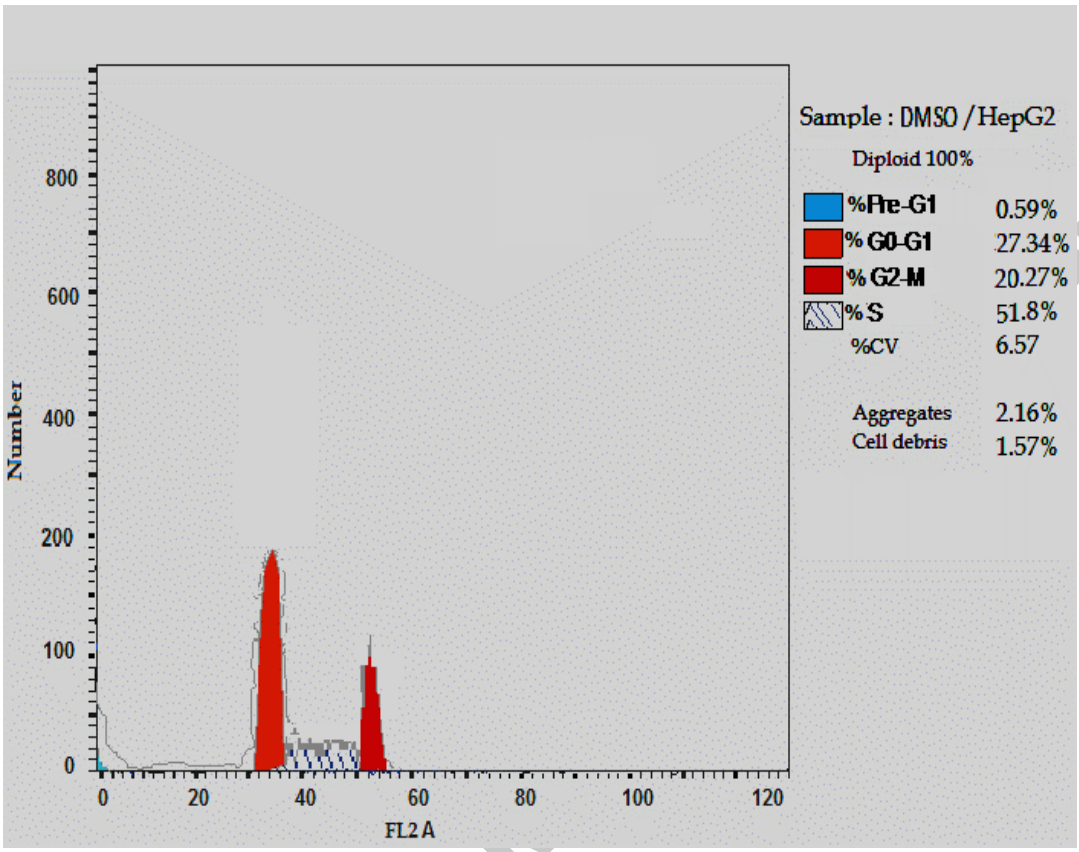

Fig. 6: Cell cycle analysis of HepG2 cells treated with DMSO.

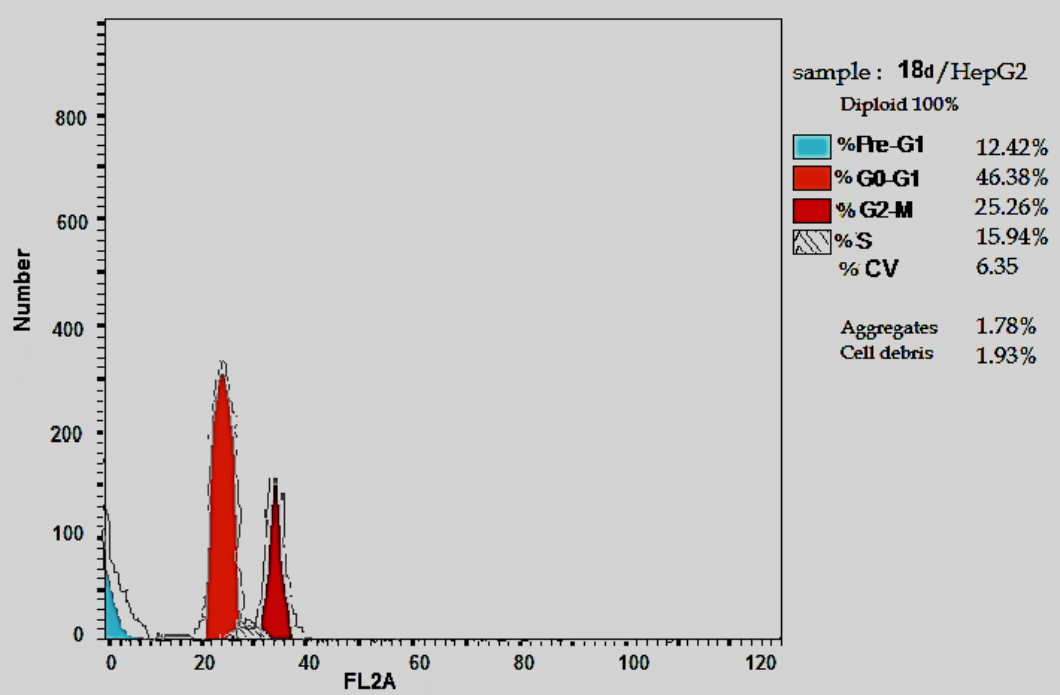

Fig. 7: Cell cycle analysis of HepG2 cells treated with compound **18_d** at 1 µM concentration

Table 3: Effect of compound **18_d** and DMSO on cell cycle of HepG2 cell line

Sample	Conc. (µM)	pre-G_1 (%)	G_0/G_1 (%)	S (%)	G_2/M (%)
18_d / HepG2	1	12.42	46.38	15.94	25.26
DMSO / HepG2	-	0.59	27.34	51.80	20.27

2.2.5. Annexin V-FITC apoptosis assay

In order to confirm the apoptosis induction, Annexin V binding studies by flow cytometer was carried out. To determine early and late apoptosis, Annexin V conjugated with FITC is used to stain cells in combination with Propidium Iodide (PI). As phosphatidyl serine externalization is the hallmark of apoptotic cells, Annexin V binds to the membrane and gives fluorescence. Thus, Annexin V stained cells represent cells with intact membranes and externalized phosphatidyl serine. Cells that stained positive for Annexin V/PI represents the cells in the late apoptotic stage that have lost membrane integrity [66].

As EGFR-TK inhibitors can induce cancer cell apoptosis [67], the apoptotic nature of compound **18_d** against HepG2 cells was evaluated via flow cytometry detection using AnnexinV-FITC and propidium iodide (PI) double staining. The results revealed that application of compound **18_d** on HepG2 cells for 48 h with increasing its concentration from 0 µM to 1 µM, increases the early apoptosis ratio (lower right quadrant of the cytogram) from 0.21% to 15.61%, and increases the late apoptosis ratio (higher right quadrant of the cytogram) from 0.12 % to 45.45%. This means that compound **18_d** induced almost up to 185 folds both early and late cellular apoptosis when compared with the control. These data suggest that compound **18_d** is good apoptotic agent **(Fig. 8 & Table 4)**.

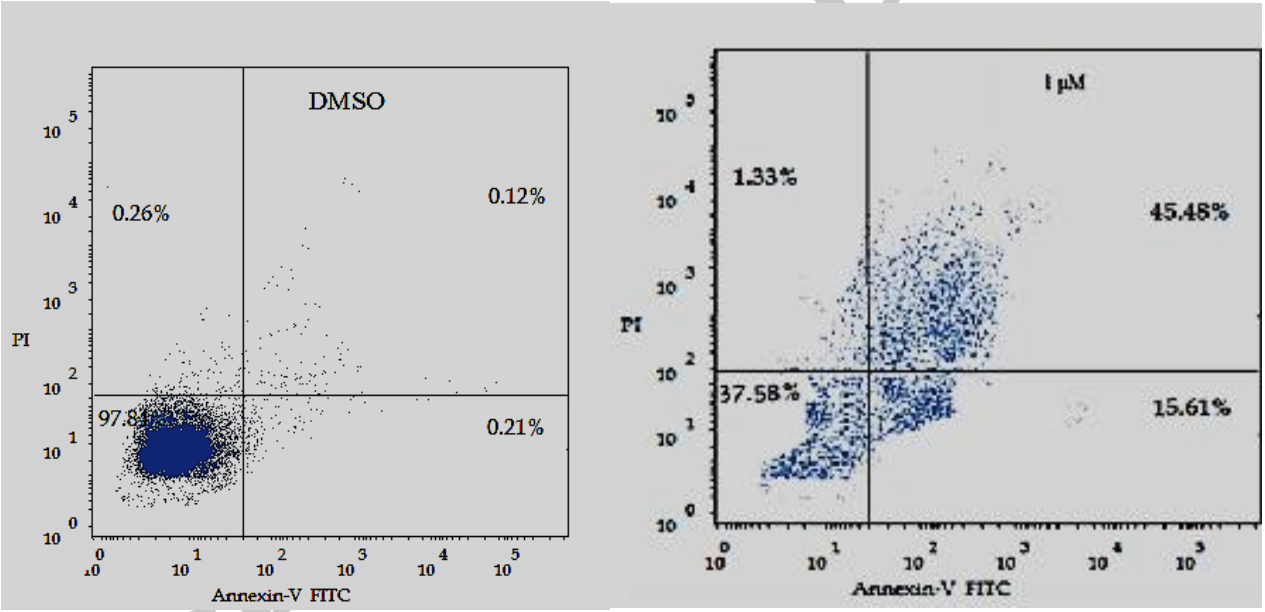

Fig. 8: Effect of compound **18_d** and DMSO on the percentage of annexin V-FITC-positive staining in HepG2 cells

Table 4: Effect of compound **18_d** and DMSO on the percentage of annexin V-FITC-positive staining in HepG2 cells.

Sample/ cell line	Concentration (µM)	Early apoptosis (%)	Late apoptosis (%)

18_d/HepG2	1	15.61	45.48
DMSO/HepG2	-	0.21	0.12

2.3.Docking studies

Additionally, the synthesized compounds were docked into the ATP binding pockets of Wild-type EGFR-TK ($EGFR^{WT}$, PDB: 4HJO) [68] and mutant EGFR-TK ($EGFR^{T790M}$, PDB: 3W2O)[69] to investigate the putative interaction mechanism with the EGFR-TK target.

The cavities of $EGFR^{WT}$ and $EGFR^{T790M}$ consist of five main parts; adenine binding pocket, hydrophilic ribose pocket, hydrophobic region I, hydrophobic region II and phosphate binding region. The adenine binding pocket is of mostly hydrophobic character. The N1 and N6 nitrogen atoms of the adenine ring of ATP are involved in a hydrogen bonding interaction with two amino acids, Gln767 and Met769, of the hinge region. The hydrophilic ribose pocket contains Cys773 residue, which is unique to the EGFR-TK and provides both potency and selectivity. The hydrophobic region I comprises Thr766 and Thr860 residues, playing a crucial role in inhibitor selectivity. The hydrophobic region II is formed by Leu694 and Gly772 residues. The phosphate binding region has high solvent exposure and is not of primary importance with respect to binding affinity [41, 42]. (**Fig. 1**).

To date, several $EGFR^{T790M}$ inhibitors have been developed to target Cys797 residue located at the lip of the adenosine triphosphate (ATP)-binding cleft and Met793 of the hinge region. These compounds were rationally designed to make a covalent bond with C797, which provides the potential to inhibit $EGFR^{T790M}$ mutation [69].

The results of docking studies against the $EGFR^{WT}$ revealed that the synthesized compounds have similar orientations inside the ATP binding site. The designed compounds gave good binding energies ranging from - 16.90 to - 26.96 kcal/mol (**Table 5**).

The binding mode of the co-crystallized ligand, erlotinib, exhibited an energy binding of - 25.17 kcal/mol. Quinazoline nucleus was oriented in the adenine pocket of the receptor, The N1 atom of pyrimidine ring formed a hydrogen bond with Met769 with a distance of 2.17A˚. The phenyl ring formed pi-sigma interaction with Lue694. The ethynylphenyl moiety occupied the hydrophobic pocket I forming pi-cation interaction

with Lys721, and hydrophobic interaction with Thr766, Thr830, Ala719, Lue764, Ile720 and Ile765 residues. Besides, the bis (2-methoxyethoxy) groups occupied the hydrophobic region II forming hydrophobic interaction with Leu694 and Gly772 residues (**Fig 9**).

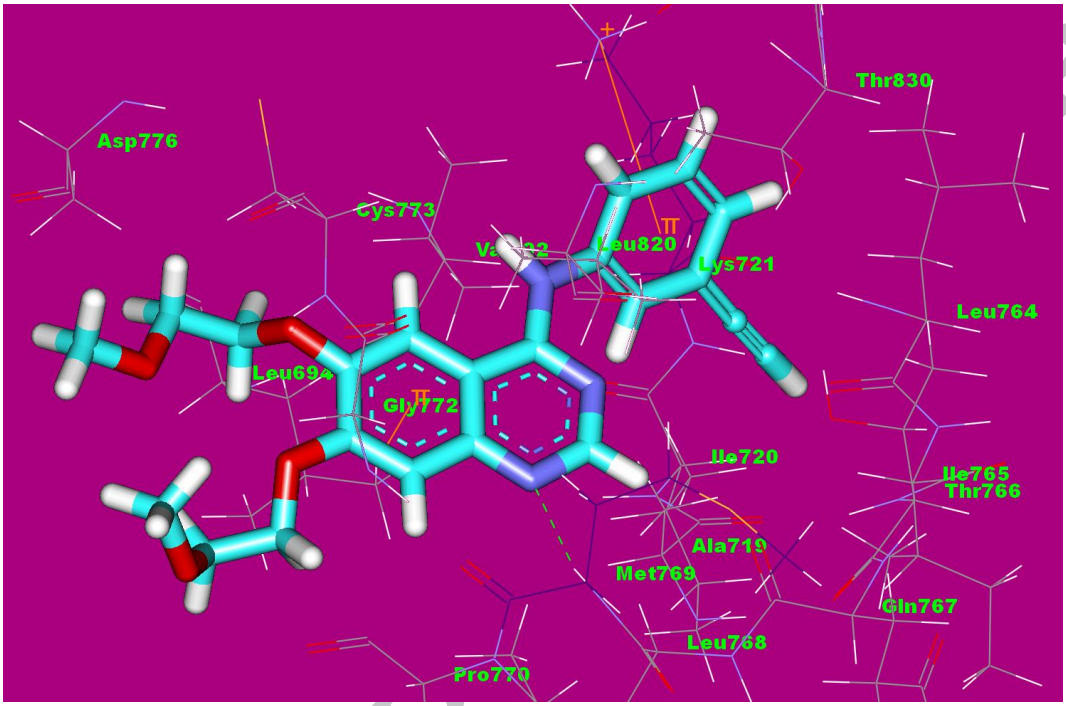

Fig. 9: Erlotinib docked into the active site of $EGFR^{WT}$ formed one hydrogen bond (green) with Met769 residue. The hydrophobic interactions are represented in orange lines.

Compound **15_b** as a representative example showed a binding mode as like as that of erlotinib, with affinity value of - 24.78 kcal/mol. The 1*H*-pyrazolo[3,4-*d*]pyrimidine moiety was oriented in the adenine pocket of the receptor. The two nitrogen atoms of hydrazone moiety formed two hydrogen bonds with Met769 with a distance of 1.58 and 2.19 A˚. The hydroxyphenyl moiety occupied the hydrophobic pocket I forming hydrophobic interactions with Ala719, Lue820 and Val 702 residues, while the hydroxyl group formed two hydrogen bonds with Thr766 and Thr830 with a distance of 2.32 and 2.04A˚, respectively. Moreover, the phenyl group at position-6 occupied the hydrophobic

region II forming pi-cation interaction with Lys704, and hydrophobic interaction with Leu694 Gly772 and Pro770 residues (**Fig 10 & 11**).

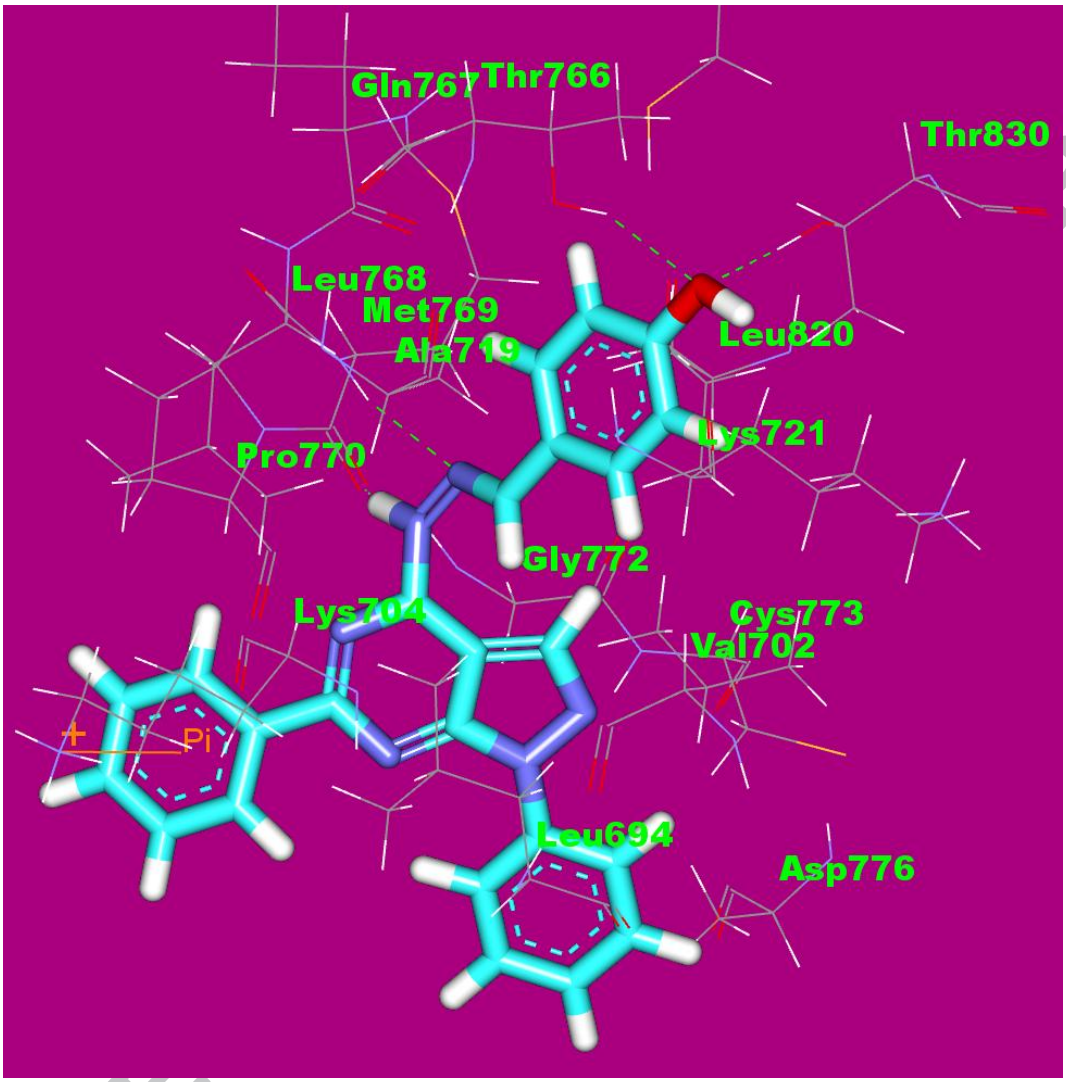

Fig. 10: Compound **15_b** docked into the active site of $EGFR^{WT}$ formed four hydrogen bonds (green) with Met769, Thr766, Thr766 and Thr830, residues. The pi interactions are represented in orange lines.

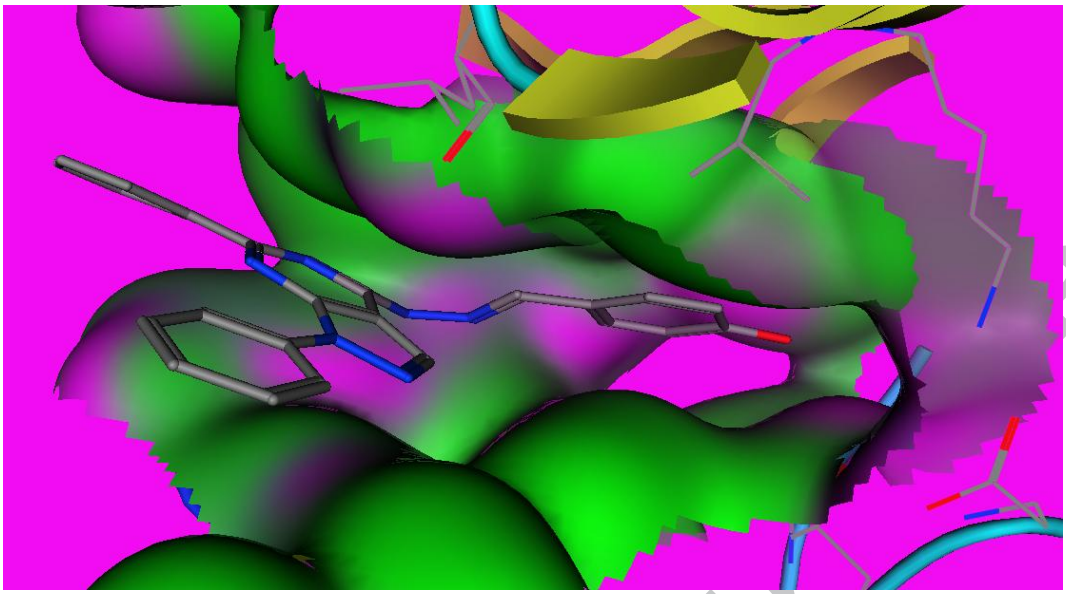

Fig. 11: Mapping surface showing compound **15_b** occupying the active pocket of $EGFR^{WT}$.

The binding mode of compound **18_d** was as like as that of erlotinib, with affinity value of - 24.93 kcal/mol. The 1*H*-pyrazolo[3,4-*d*]pyrimidine moiety occupied the adenine binding site forming a hydrogen bond with Lys721 with a distance of 1.64 A˚. The two nitrogen atoms of ketohydrazinyl group moiety formed two hydrogen bonds with Asp831 and Thr830 with a distance of 1.56 and 1.87A˚, respectively. The fluoro phenyl moiety occupied the hydrophobic pocket I forming hydrophobic interactions with Phe832, Lue843, Lue764, Lue753 and Thr766 residues. In addition, the phenyl group at position-6 occupied the hydrophobic region II (**Fig 12 & 13**).

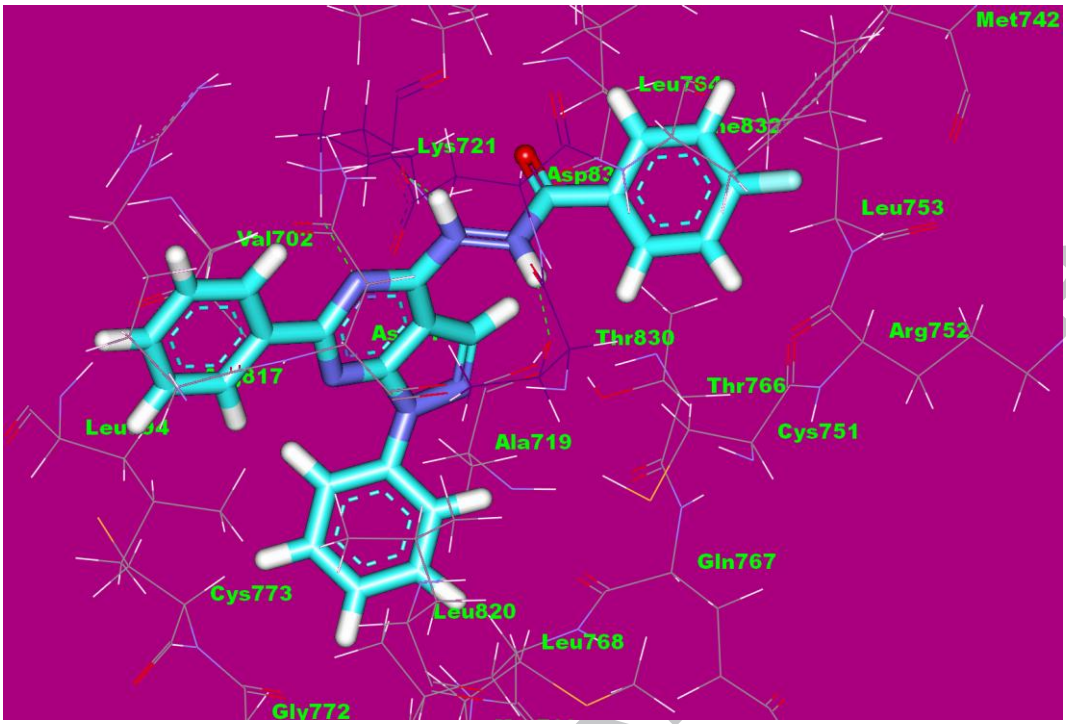

Fig. 12: Compound **18$_d$** docked into the active site of EGFR^{WT} formed three hydrogen bonds (green) with Lys721, Asp831 and Thr830 residues. The pi interactions are represented in orange lines.

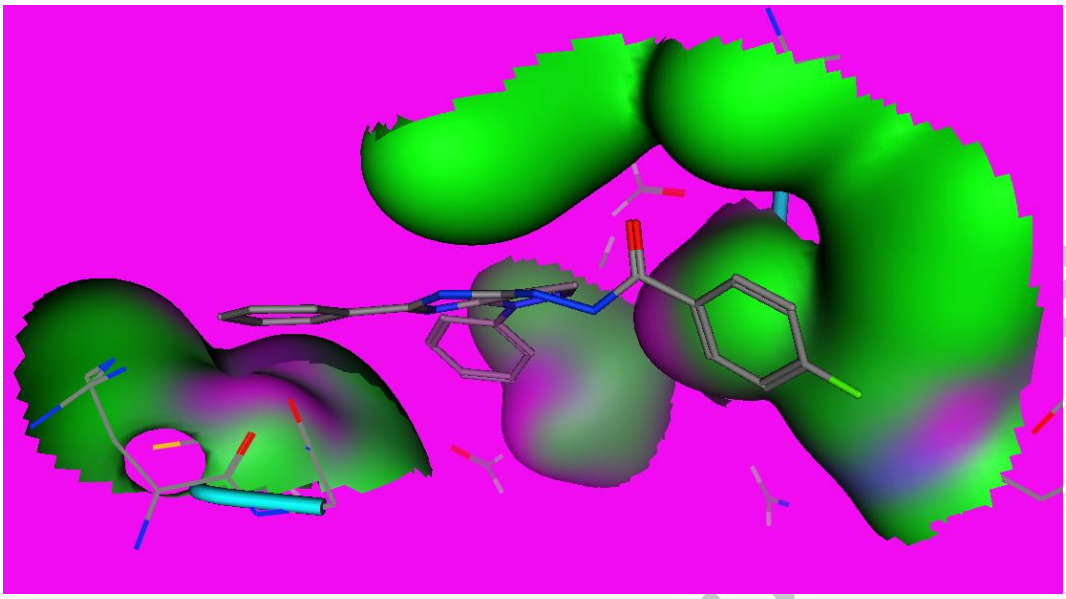

Fig. 13: Mapping surface showing compound **18_d** occupying the active pocket of $EGFR^{WT}$.

The results of docking studies against the mutant EGFR-TK ($EGFR^{T790M}$) revealed that the synthesized compounds have similar orientations inside the ATP binding site. Osimertinib and TAK-285(co-crystallized ligand) were used as reference ligands. The designed compounds gave good binding energies ranging from - 19.27 to - 27.46 kcal/mol (**Table 5**).

The binding mode of the co-crystallized ligand, TAK-285, showed an energy binding of - 27.35 kcal/mol. Pyrrolo[3,2-*d*]pyrimidine moiety was oriented in the adenine pocket of the receptor forming pi-sigma interaction with Leu844 and Ala743. The N1 atom of pyrimidine ring formed a hydrogen bond with Met793 with a distance of 2.23 A˚. The 3-(trifluoromethyl)phenoxy group occupied the hydrophobic region I forming hydrophobic interaction with Ile759 and Lys745. One fluoro atom of trifluoromethane moiety formed one hydrogen bond with Lys745 with a distance of 1.41 A˚. The *N*-ethyl-3-hydroxy-3-methylbutanamide moiety occupied the hydrophobic pocket II. The hydroxyl group formed a hydrogen bond with Ser720 with a distance of 1.79 A˚. The central phenyl moiety formed pi-sigma interaction with Lys745, Val726 and Met790 (**Fig 14**).

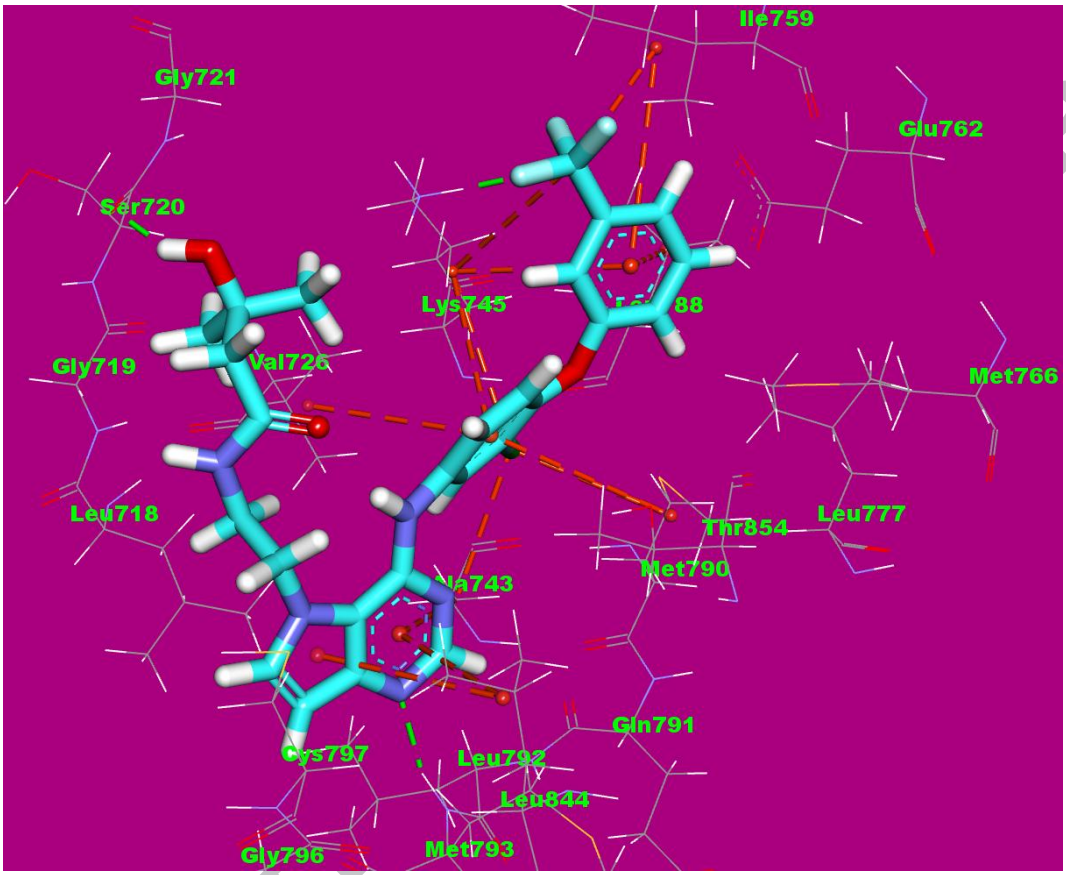

Fig. 14: Co-crystallized ligand (TAK-285) docked into the active site of EGFR^{T790M}, the hydrogen bonds are represented in green dashed lines and the pi interactions are represented in orange dashed lines

Compound **17$_d$** as a representative example showed a binding mode as like as that of co-crystalized ligand, TAK-285, with affinity value of - 26.50 kcal/mol. The 1*H*-pyrazolo [3,4-*d*]pyrimidine moiety was oriented in the adenine binding pocket forming pi-sigma interactions with Leu844, Met793, Leu718 and Ala743. Also, N2 atom of pyrazole moiety formed one hydrogen bond with Met793 with a distance of 1.95 A˚. The cyclohexyl moiety occupied the hydrophobic pocket I forming hydrophobic interactions with Lys745. Moreover, the phenyl group at position-6 occupied the hydrophobic region II forming pi-sigma interactions with Cys797 and Leu844 (**Fig 15**).

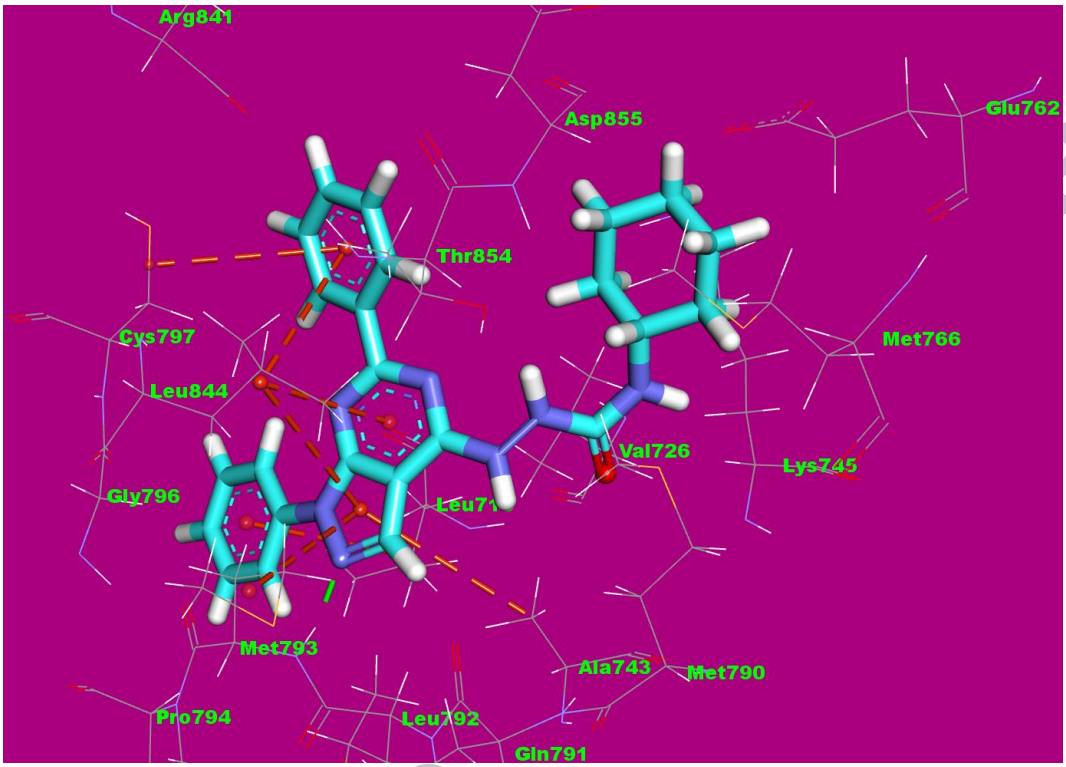

Fig. 15: Binding of compound **17$_d$** with EGFR^{T790M}, the hydrogen bonds are represented in green dashed lines and the pi interactions are represented in orange dashed lines.

The binding mode of compound **18$_d$** was as like as that of TAK-285, with affinity value of - 27.13 kcal/mol. The 1*H*-pyrazolo[3,4-*d*]pyrimidine moiety occupied the adenine binding site forming pi-sigma interactions with Leu844, Leu718, Met793 and Ala743. N2 atom of pyrazole moiety formed one hydrogen bond with Met793 with a distance of 2.21 A˚. The 4-fluorophenyl moiety occupied the hydrophobic pocket I forming hydrophobic interactions with Lys745. Moreover, the phenyl group at position-6 occupied the hydrophobic region II forming pi-sigma interaction with Cys797 (**Fig 16**).

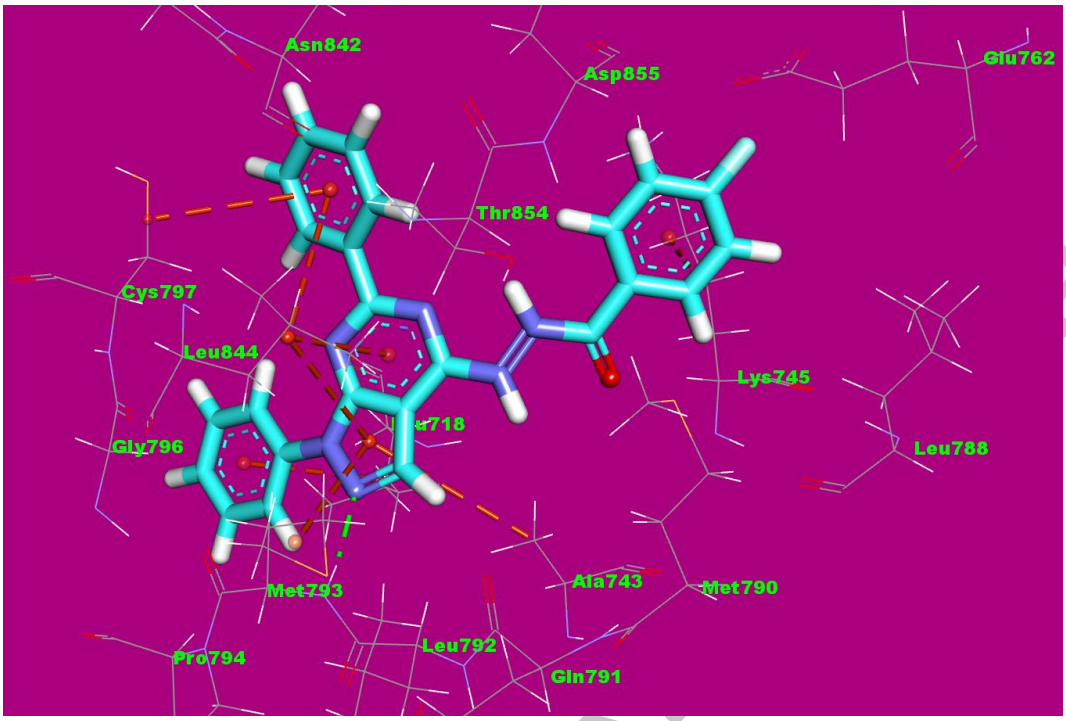

Fig. 16: Binding of compound **18$_d$** with EGFR^{T790M}, the hydrogen bonds are represented in green dashed lines and the pi interactions are represented in orange dashed lines.

Table 5: The docking binding free energies of the synthesized compounds against EGFR^{WT} and EGFR^{T790M}

Comp.	Binding free energy (kcal/mol)	
	EGFR^{WT}	EGFR^{T790M}
14	- 16.90	- 19.27
15$_a$	- 25.48	- 22.30
15$_b$	- 24.78	- 22.43
15$_c$	- 22.87	- 26.49
15$_d$	- 21.70	- 22.61
15$_e$	- 22.13	- 26.51
15$_f$	- 24.37	- 22.77
15$_g$	- 23.04	- 26.89
15$_h$	- 25.33	- 24.21
15$_i$	- 22.01	- 21.50

15_j	- 23.53	- 26.81
15_k	- 20.48	- 24.60
15_l	- 23.51	- 25.15
15_m	- 22.90	- 23.36
15_n	- 25.19	- 22.01
15_o	- 24.33	- 23.70
16	- 25.63	- 23.44
17_a	- 22.98	- 21.37
17_b	- 24.32	- 24.21
17_c	- 19.06	- 22.30
17_d	- 20.67	- 26.50
17_e	- 19.40	- 23.26
17_f	- 20.86	- 26.95
18_a	- 20.03	- 26.86
18_b	- 25.03	- 27.20
18_c	- 26.96	- 27.46
18_d	- 24.93	- 27.13
18_e	- 24.89	- 26.68
19	- 20.55	- 24.13
20	- 17.09	- 21.55
Erlotinib	- 25.17	-
TAK-285	-	- 27.35
Osimertinib	-	- 27.01

3. Structure-activity relationships (SAR)

Observing the results of biological tests, valuable data about the structure-activity relationships of 1*H*-pyrazolo[3,4-*d*]pyrimidine derivatives as potential EGFR-TK inhibitors could be deduced.

Initially, the effect of linker lengths on the activity against $EGFR^{WT}$ was explored. It was found that a linker with three atoms is advantageous. Comparing the activities of

compounds **18_a (**ketohydrazinyl linker, IC_{50} = 1.87 ± 0.32 µM), **15_k (**acetohydrazonoyl linker, IC_{50} = 1.02 ± 0.41 µM) and **15_a (**methylenehydrazinyl linker, IC_{50} = 4.91 ± 0.61 µM) with incorporated unsubstituted phenyl moiety, indicated that the ketohydrazinyl linker was more active than acetohydrazonoyl linker, and the latter was more active than methylenehydrazinyl one.

With regard to the four atoms linker, the decreased IC_{50} values of derivatives incorporating semicarbazide linker as compounds **$17_{b,d,f}$** (IC_{50} = 0.29 ± 0.14, 0.26 ± 0.14 and 0.32 ± 0.20 µM, respectively) than the corresponding members of thiosemicarbazide one as compounds **$17_{a,c,e}$** (IC_{50} = 0.35 ± 0.21, 0.44 ± 0.24 and 0.56 ± 0.19 µM, respectively), indicated that semicarbazide linker is more advantageous than thiosemicarbazide one.

Then, the impact of the substitution on the terminal hydrophobic head was investigated. The increased IC_{50} value of compounds **15_a** (IC_{50} = 4.91 ± 0.61 µM) with incorporated unsubstituted phenyl moiety, than those of their corresponding members **15_{b-g}** (IC_{50} = 0.19 ± 0.13, 0.49 ± 0.10, 1.84 ± 0.19, 0.23 ± 0.31, 0.44 ± 0.29 and 0.28 ± 0.22 µM) with 4- substituted phenyl moiety, indicated that substitution on phenyl group is advantageous.

With regard to the effect of substitution in these members, the activities were decreased in the order of 4-OH > 4-NO_2 > 2,6-Cl > 4-Cl > 4-OCH_3 > 4-CH_3. Interestingly, the introduction of thiophenyl and naphthyl functionalities afforded compounds **15_i** (IC_{50} = 0.51 ± 0.23) and **15_j** (IC_{50} = 0.16 ± 0.11), respectively, with superior inhibitory activities comparable to compound **15_a** (IC_{50} = 4.91 ± 0.61) with unsubstituted phenyl moiety.

4. Conclusion

In summary, thirty 1*H*-pyrazolo[3,4-*d*]pyrimidine derivatives (**15_{a-o}, 16, 17, $_{a-f}$, 18_{a-e}, 19** and **20**) were designed and synthesized. The synthesized compounds were evaluated for their inhibitory action against $EGFR^{WT}$, and compared with erlotinib as a positive control. In this study, most of the synthesized compounds showed $EGFR^{WT}$ inhibitory effect higher than erlotinib as compounds **15_b, 15_e, 15_g, 15_h, 15_j, 15_n, 15_o, 17_a, 17_b, 17_d, 17_f, 18_d** and **18_e** with IC_{50} values ranging from 0.09 ± 0.11 to 0.41 ± 0.21 µM.

The SAR studies pointed that, substitution on the terminal hydrophobic head seems to be preferred. Also, it was found that the linker with three atoms is advantageous. Thirteen compounds that exhibited promising IC_{50} values against $EGFR^{WT}$ were further evaluated *in vitro* for their inhibitory activities against mutant $EGFR^{T790M}$. Compounds **17_d** (IC_{50} = 2.72 ± 0.21 nM) and **17_f** (IC_{50} = 3.90 ± 0.33 nM) showed excellent inhibitory activities towards $EGFR^{T790M}$. Also, these compounds were tested for their anti-proliferative activities against three cancer cell lines bearing $EGFR^{WT}$ (MCF-7, HepG2, A549), and two cancer cell lines bearing $EGFR^{T790M}$ (H1975 and HCC827). Compounds **15_g, 15_j, 15_n, 18_d** and **18_e** were the most potent anticancer agents against the $EGFR^{WT}$ containing cells, while compounds**15_e**, **17_d** and **17_f** showed promising anti-proliferative activities against $EGFR^{T790M}$ containing cells. In addition, the most active compound **18_d** was tested for its effect on cell cycle progression and induction of apoptosis in the HepG2 cell line. It was found that it has apoptotic effect and can arrest G_0/ $G_1$and G_2/M phases of cell cycle. Also, molecular docking studies was carried out to recognize the binding pattern of the synthesized compounds $EGFR^{WT}$ and $EGFR^{T790M}$. The synthesized compounds showed good binding energies and correct binding modes. Therefore, compounds **15_b**, **17_d** and **18_d** can be considered as interesting candidates for further development of more potent anticancer agents.

5. Experimental

5.1. Chemistry

5.1.1. General

Melting points were measured on a Gallen-kamp melting point apparatus and were uncorrected. The IR spectra were recorded on Nikolet IR 200 FT IR spectrophotometer using KBr discs (λ max in cm^{-1}). ^1H NMR and ^{13}C NMR spectra were performed on Gemini 300BB spectrometer at 300 MHz and Bruker spectrometer at 100 MHz, respectively. TMS was used as internal standard and DMSO-d_6 as solvent. The chemical shifts were reported in ppm (δ) and coupling constant (J) values were given in Hertz (Hz). Signal multiplicities were represented by s (singlet), d (doublet), t (triplet), q (quadruplet), and m (multiplet). All of the new compounds were analyzed for C, H and N

and agreed with the proposed structures within ± 0.4% of the theoretical values by the automated CHN analyzer. Mass spectra were recorded on a unit of Shimadzu GCMS-QP/MS-QP5050A spectrometer operating at 70 ev. The purity of the compounds was checked by thin layer chromatography (TLC) using Merck silica gel 60 F254 recoated sheets. Compounds **9, 10, 11, 12** and **13** were prepared according to the reported procedures [29, 49-52].

5.1.2. *4-Hydrazinyl-1,6-diphenyl-1H-pyrazolo[3,4-d]pyrimidine 14*

A mixture of 4-chloro-1,6-diphenyl-1*H*-pyrazolo[3,4-*d*]pyrimidine **13** (3.06 g, 0.01 mol) and hydrazine hydrate (99%, 5 mL, 0. 1 mol) were heated under reflux for 8 h. After cooling, the formed solid was collected by filtration, washed with hot ethanol (95%, 10 mL), and crystallized from isopropanol to yield the desired product **14**.

Yellow solid (2.2 g, 73%); m.p. 236 - 238 °C; IR (KBr, *v*, cm^{-1}): 3320 - 3310 (NH_2), 3190 (NH), 3082 (Ar-H); ^{1}H NMR (DMSO-d_6, 300 MHz): 4.73 (s, 2H, NH_2, exchanged with D_2O), 7.44 (t, 1H, *J* = 7.50 Hz, Ar-H), 7.69 (t, 1H, *J* = 6.40 Hz, Ar-H), 7.83 (t, 2H, *J* = 7.50 Hz, Ar-H), 8.11 (t, 2H, *J* = 6.40 Hz, Ar-H), 8.26 (d, 2H, *J* = 8.80 Hz, Ar-H), 8.48 (d, 2H, *J* = 9.20 Hz, Ar-H), 8.83 (s, 1H, Ar-H C3-H pyrazole), 9.89 (s, 1H, NH, exchanged with D_2O); MS (*m/z*): 302 (M^+, 8.95%), 271 (100%); Anal. Calcd. for $C_{17}H_{14}N_6$ **(**302): C, 67.54; H, 4.67; N, 27.80. Found: C, 67.51; H, 4.65; N, 27.78.

5.1.3. General procedure for preparation of compounds15$_{a-o}$

A mixture of hydrazide derivative **14** (0.30 g, 0.001 mol), appropriate aromatic aldehydes or acetophenones (0.001 mol) and catalytic amount of glacial acetic acid (0.5 mL) was heated under reflux in absolute ethanol (20 mL) for specific time. The precipitate that formed on hot was filtered and crystallized from ethanol to yield the title compounds **15$_{a-o}$**.

5.1.3.1. *4-(2-Benzylidenehydrazinyl)-1,6-diphenyl-1H-pyrazolo[3,4-d]pyrimidine* **15$_a$**

Yellowish white solid; reaction time:1 h, yield 90% (0.35 g), m.p. 230 - 232°C; IR (KBr, *v*, cm^{-1}): 3210 (NH), 3052 (Ar-H). ^{1}H NMR (DMSO-d_6, 300 MHz): 7.44 (t, 1H, *J* = 7.20 Hz, Ar-H), 7.59 (t, 1H, *J* = 5.50 Hz, Ar-H), 7.60 (t, 1H, *J* = 8.10 Hz, Ar-H), 7.63 (t, 2H, *J* = 7.20 Hz, Ar-H), 7.69 (t, 2H, *J* = 5.50 Hz, Ar-H), 8.30 (t, 2H, *J* = 8.10 Hz, Ar-H), 8.33 (d, 2H, *J* = 6.30 Hz, Ar-H), 8.48 (d, 2H, *J* = 9.20 Hz, Ar-H), 8.51 (d, 2H, *J* = 7.80 Hz, Ar-H), 8.61 (s, 1H, CH=N), 8.73 (s, 1H, Ar-H, C3–H pyrazole), 11.80 (s, 1H, NH, exchanged with D_2O); ^{13}C NMR (DMSO, 100 MHz): 102.63, 119.54, 120.04, 121.21, 123.14, 124.07, 125.09, 127.44, 128.81, 129.72, 131.66, 133.57, 135.09, 138.50, 145.96, 152.82, 154.90, 156.59; MS (*m/z*): 390 (M^+, 5.24%), 313 (100%); Anal. Calcd. for $C_{24}H_{18}N_6$ **(**390): C, 73.83; H, 4.65; N, 21.52. Found: C, 73.85; H, 4.68; N, 21.49.

5.1.3.2. *4-[2-(4-Hydroxybenzylidene)hydrazinyl]-1,6-diphenyl-1H-pyrazolo[3,4-d]pyrimidine* 15_b

White powder; reaction time: 1.5 h; yield 92% (0.37 g), m.p. 222 - 224°C. IR (KBr, *v*, cm^{-1}): 3420 (br, OH), 3205 (NH), 3077 (Ar-H). ^{1}H NMR (DMSO-d_6, 300 MHz): 7.41 (d, 2H, *J* = 7.20 Hz, Ar-H), 7.61 (t, 1H, *J* = 7.50 Hz, Ar-H), 7.66 (t, 1H, *J* = 8.10 Hz, Ar-H), 8.00 (t, 2H, *J* = 7.50 Hz, Ar-H), 8.10 (t, 2H, *J* = 8.10 Hz, Ar-H), 8.11 (d, 2H, *J* = 7.20 Hz, Ar-H), 8.12 (d, 2H, *J* = 8.60 Hz, Ar-H), 8.28 (d, 2H, *J* = 6.10 Hz, Ar-H), 8.57 (s, 1H, CH=N), 8.79 (s, 1H, Ar-H, C3–H pyrazole), 9.89 (s, 1H, OH, exchanged with D_2O), 11.55 (s, 1H, NH, exchanged with D_2O); ^{13}C NMR (DMSO, 100 MHz): 104.78, 115.28, 121.13, 123.14, 124.07, 125.09, 127.44, 128.81, 129.72, 131.66, 133.57, 135.09, 138.50, 145.96, 152.82, 154.90, 156.59, 158.70; MS (*m/z*): 406 (M^+, 11.91%), 286 (100%). Anal. Calcd. for $C_{24}H_{18}N_6O$ **(**406): C, 70.92; H, 4.46; N, 20.68. Found: C, 70.89; H, 4.47; N, 20.66.

5.1.3.3. *4-(2-(4-Methoxybenzylidene)hydrazinyl)-1,6-diphenyl-1H-pyrazolo[3,4-d]pyrimidine* 15_c

Green solid; reaction time: 1 h; yield 93% (0.39 g); m.p. 226 - 228°C; IR (KBr, *v*, cm^{-1}): 3195 (NH), 3068 (Ar-H), 2952 (aliph-CH); ^{1}H NMR (DMSO-d_6, 300 MHz): 3.80 (s, 3H, CH_3), 7.10 (d, 2H, *J* = 6.90 Hz, Ar-H), 7.21 (t, 1H, *J* =7.80 Hz, Ar-H), 7.43 (t, 1H, *J* = 7.20 Hz, Ar-H), 7.57 (t, 2H, *J* = 7.80 Hz, Ar-H), 7.68 (t, 2H, *J* = 7.20 Hz, Ar-H), 8.32 (d,

2H, *J* = 6.90 Hz, Ar-H), 8.48 (d, 2H, *J* = 5.80 Hz, Ar-H), 8.51 (d, 2H, *J* = 9.10 Hz, Ar-H), 8.60 (s, 1H, CH=N), 8.80 (s, 1H, Ar-H, C3–H pyrazole), 11.53 (s, 1H, NH, exchanged with D_2O); ^{13}C NMR (DMSO, 100 MHz): 55.88, 104.99, 115.28, 121.82, 122.05, 127.44, 128.67, 128.83, 128.99, 129.67, 129.73, 132.44, 135.09, 138.50, 145.96, 152.82, 154.90, 156.99, 161.83; MS (*m/z*): 420 (M^+, 18.24%), 405 (100%); Anal. Calcd. for $C_{25}H_{20}N_6O$**(**420): C, 71.41; H, 4.79; N, 19.99. Found: C, 71.37; H, 4.75; N, 20.01.

5.1.3.4. *4-(2-(4-Methylbenzylidene)hydrazinyl)-1,6-diphenyl-1H-pyrazolo[3,4-d]pyrimidine* 15_d

Yellow solid; reaction time: 2 h; yield 87% (0.35 g); m.p. 216 - 218°C; IR (KBr, *v*, cm^{-1}): 3192 (NH), 3081 (Ar-H), 2971 (aliph-CH). ^1H NMR (DMSO-d_6, 300 MHz): 2.30 (s, 3H, CH_3), 7.40 (d, 2H, *J* = 7.50 Hz, Ar-H), 7.55 (t, 1H, *J* = 6.90 Hz, Ar-H), 7.62 (t, 1H, *J* = 8.40 Hz, Ar-H), 7.67 (t, 2H, *J* = 6.90 Hz, Ar-H), 8.27 (t, 2H, *J* = 8.40 Hz, Ar-H), 8.30 (d, 2H, *J* = 7.50 Hz, Ar-H), 8.42 (d, 2H, *J* = 9.10 Hz, Ar-H), 8.44 (d, 2H, *J* = 6.30 Hz, Ar-H), 8.55 (s, 1H, CH=N), 8.67 (s, 1H, Ar-H, C3–H pyrazole), 11.69 (s, 1H, NH, exchanged with D_2O); ^{13}C NMR (DMSO, 100 MHz): 27.67, 102.63, 121.21, 121.32, 123.14, 124.07, 125.09, 127.44, 128.81, 129.72, 131.66, 133.57, 135.09, 138.50, 140.79, 145.96, 152.80, 154.62, 156.04; MS (*m/z*): 404 (M^+, 9.64%), 313 (100%). Anal. Calcd. for $C_{25}H_{20}N_6$ **(**404): C, 74.24; H, 4.98; N, 20.78. Found: C, 74.22; H, 4.95; N, 20.82.

5.1.3.5.*4-(2-(4-Nitrobenzylidene)hydrazinyl)-1,6-diphenyl-1H-pyrazolo[3,4-d]pyrimidine* 15_e

Orange solid; reaction time: 9 h; yield 81% (0.35 g); m.p. 243-245°C; IR (KBr, *v*, cm^{-1}): 3199 (NH), 3091 (Ar-H). ^1H NMR (DMSO-d_6, 300 MHz): 7.40 (t, 1H, *J* =6.30 Hz, Ar-H), 7.54 (t, 1H, *J* =7.50 Hz, Ar-H), 7.57 (t, 2H, *J* = 6.30 Hz, Ar-H), 7.62 (t, 2H, *J* = 7.50 Hz, Ar-H), 7.67 (d, 2H, *J* = 8.70 Hz, Ar-H), 8.27 (d, 2H, *J* = 8.70 Hz, Ar-H), 8.42 (d, 2H, *J* = 8.40 Hz, Ar-H), 8.55 (d, 2H, *J* = 9.40 Hz, Ar-H), 8.58 (s, 1H, CH=N), 8.67 (s, 1H, Ar-H, C3–H pyrazole), 11.92 (s, 1H, NH, exchanged with D_2O); ^{13}C NMR (DMSO, 100 MHz): 97.87, 121.13, 122.71, 123.14, 126.77, 128.87, 129.60, 131.22, 131.66, 132.44, 133.57, 135.09, 138.50, 145.96, 150.13, 153.53, 155.04, 157.59; MS (*m/z*): 435

(M^+, 3.64%), 77 (100%); Anal. Calcd. for $C_{24}H_{17}N_7O_2$ **(**435): C, 66.20; H, 3.94; N, 22.52. Found: C, 66.24; H, 3.91; N, 22.56.

5.1.3.6. *4-(2-(4-Chlorobenzylidene)hydrazinyl)-1,6-diphenyl-1H-pyrazolo[3,4-d]pyrimidine* 15_f

White solid; reaction time: 4 h; yield 79% (0.33 g); m.p. 233 - 235°C; IR (KBr, *v*, cm^{-1}): 3222 (NH), 3081 (Ar-H). ^{1}H NMR (DMSO-d_6, 300 MHz): 7.43 (d, 2H, *J* = 7.50 Hz, Ar-H), 7.50 (t, 1H, *J* =11.40 Hz, Ar-H), 7.55 (t, 1H, *J* =5.70 Hz, Ar-H), 7.62 (t, 2H, *J* = 11.40 Hz, Ar-H), 8.17 (t, 2H, *J* = 5.70 Hz, Ar-H), 8.29 (d, 2H, *J* = 7.50 Hz, Ar-H), 8.41 (d, 2H, *J* = 7.20 Hz, Ar-H), 8.55 (d, 2H, *J* = 8.10 Hz, Ar-H), (s, 1H, CH=N), 8.77 (s, 1H, Ar-H, C3–H pyrazole), 11.78 (s, 1H, NH, exchanged with D_2O); ^{13}C NMR (DMSO, 100 MHz): 102.99, 116.95, 121.47, 123.14, 124.66, 125.87, 127.44, 128.88, 129.70, 131.68, 133.53, 135.08, 138.52, 145.96, 152.81, 154.95, 156.57, 159.13; MS (*m/z*): 426 (M^++2, 5.01%), 424 (M^+, 15.04%), 153 (100%); Anal. Calcd. for $C_{24}H_{17}ClN_6$ **(**424): C, 67.84; H, 4.03; N, 19.78. Found: C, 67.81; H, 4.07; N, 19.75.

5.1.3.7. *4-(2-(2,6-Dichlorobenzylidene)hydrazinyl)-1,6-diphenyl-1H-pyrazolo[3,4-d]pyrimidine* 15_g

Red solid; reaction time: 6 h; yield 83% (0.38 g); m.p.: 255-257°C; IR (KBr, *v*, cm^{-1}): 3232 (NH), 3088 (Ar-H). ^{1}H NMR (DMSO-d_6, 300 MHz): 7.10 (t, 1H, *J* = 6.00 Hz, Ar-H), 7.21 (d, 2H, *J* =6.00 Hz, Ar-H), 7.43 (t, 1H, *J* =7.50 Hz, Ar-H), 7.54 (t, 1H, *J* = 8.10 Hz, Ar-H), 7.59 (t, 2H, *J* = 7.50 Hz, Ar-H), 8.28 (t, 2H, *J* = 8.10 Hz, Ar-H), 8.31 (d, 2H, *J* = 9.50 Hz, Ar-H), 8.49 (d, 2H, *J* = 5.10 Hz, Ar-H), (s, 1H, CH=N), 8.80 (s, 1H, Ar-H, C3–H pyrazole), 12.03 (s, 1H, NH, exchanged with D_2O); ^{13}C NMR (DMSO, 100 MHz): 105.16, 113.54, 120.04, 120.63, 120.94, 125.09, 126.44, 128.12, 129.77, 131.66, 133.57, 135.09, 139.80, 144.58, 151.92, 154.91, 155.96, 158.16; MS (*m/z*): 462 (M^++4, 0.30%), 460 (M^++2, 1.82%), 458 (M^+, 2.72%), 186 (100%); Anal. Calcd. for $C_{24}H_{16}Cl_2N_6$ **(**458): C, 62.76; H, 3.51; N, 18.30. Found: C, 62.72; H, 3.54; N, 18.33.

5.1.3.8. 4-(2-(Cinnamylidene)hydrazinyl)- 1,6-diphenyl- 1H-pyrazolo[3,4-d] pyrimidine 15_h

Orange needle, reaction time: 5 h; yield 95% (0.39 g); m.p.: 241- 243°C; IR (KBr, *v*, cm^{-1}): 3189 (NH), 3083 (Ar-H). ^{1}H NMR (DMSO-d_6, 300 MHz): 7.50 (t, 1H, *J* = 8.40 Hz, Ar-H), 7.76 (t, 2H, *J* = 8.40 Hz, Ar-H), 7.89 (t, 1H, *J* = 7.30 Hz, Ar-H), 7.92 (t, 1H, *J* = 7.20 Hz, Ar-H), 8.06 (t, 2H, *J* = 7.30 Hz, Ar-H), 8.11 (t, 2H, *J* = 7.20 Hz, Ar-H), 8.23 (d, 2H, *J* = 5.40 Hz, Ar-H), 8.34 (d, 2H, *J* = 9.30 Hz, Ar-H), 8.40 (d, 2H, *J* = 9.50 Hz, Ar-H), 8.45 (d, 1H, *J* = 7.5 Hz, CH=C**H**-ph), 8.54 (d, 1H, *J* = 7.5 Hz, N=CH-C**H**=CH) 8.69 (s, 1H, N=CH), 8.84 (s, 1H, Ar-H, C3–H pyrazole), 11.78 (s, 1H, NH, exchanged with D_2O). ^{13}C NMR (DMSO, 100 MHz): 100.30, 119.50, 120.07, 121.22, 123.18, 124.05, 125.09, 126.67, 127.47, 128.80, 129.75, 131.61, 133.58, 134.44, 135.08, 138.52, 145.96, 152.82, 154.90, 156.59. MS (*m/z*): 416 (M^+, 16.81%), 145 (100%). Anal. Calcd. for $C_{26}H_{20}N_6$ **(**416): C, 74.98; H, 4.84; N, 20.18. Found: C, 74.95; H, 4.87; N, 20.15

5.1.3.9. *4-(2-(Thiophen-2-ylmethylene)hydrazinyl)-1,6-diphenyl-1H-pyrazolo[3,4-d]pyrimidine 15$_i$*

White solid; reaction time: 3 h yield 88% (0.34 g); m.p.: 233-235°C; IR (KBr, *v*, cm^{-1}): 3195 (NH), 3087 (Ar-H). ^{1}H NMR (DMSO-d_6, 300 MHz): 7.38 (t, 1H, *J* = 8.40 Hz, Ar-H), 7.59 (t, 1H, *J* = 5.80 Hz, Ar-H), 7.61 (t, 1H, *J* = 6.20 Hz, Ar-H), 7.64 (t, 2H, *J* = 5.80 Hz, Ar-H), 7.70 (t, 2H, *J* = 6.20 Hz, Ar-H), 7.98 (d, 1H, *J* = 6.50 Hz, Ar-H), 8.09 (d, 2H, *J* = 8.80 Hz, Ar-H), 8.65 (d, 2H, *J* = 9.10 Hz, Ar-H), 8.77 (d, 1H, *J* = 8.40 Hz, Ar-H), 8.84 (s, 1H, CH=N), 9.43 (s, 1H, Ar-H, C3–H pyrazole), 11.82 (s, 1H, NH, exchanged with D_2O); ^{13}C NMR (DMSO, 100 MHz): 102.69, 120.54, 121.91, 124.74, 125.63, 127.41, 128.81, 129.23, 130.02, 131.66, 133.51, 135.90, 138.05, 145.91, 147.96, 152.81, 154.90, 156.59. MS (*m/z*): 396 (M^+, 5.09%), 125 (100%). Anal. Calcd. for $C_{22}H_{16}N_6S$ **(**396): C, 66.65; H, 4.07; N, 21.20. Found: C, 66.62; H, 4.04; N, 21.17.

5.1.3.10. *4-(2-(Naphthalen-1-ylmethylene)hydrazinyl)-1,6-diphenyl-1H-pyrazolo[3,4-d] pyrimidine 15$_j$*

Light brown solid; reaction time: 8 h; yield 91% (0.40 g); m.p.: 251 - 253°C; IR (KBr, *v*, cm^{-1}): 3233 (NH), 3095 (Ar-H). ^{1}H NMR (DMSO-d_6, 300 MHz): 7.13 (t, 1H, *J* = 5.40 Hz, Ar-H), 7.16 (t, 1H, *J* = 9.30 Hz, Ar-H), 7.29 (t, 2H, *J* = 5.40 Hz, Ar-H), 7.33 (t, 2H, *J* = 9.30 Hz, Ar-H), 7.36 (t, 1H, *J* = 8.50 Hz, Ar-H), 7.48 (t, 1H, *J* = 8.50 Hz, Ar-H), 7.66

(t, 1H, *J* = 5.80 Hz, Ar-H), 7.69 (d, 2H, *J* = 6.50 Hz, Ar-H), 8.27 (d, 2H, *J* = 9.50 Hz, Ar-H), 8.37 (d, 2H, *J* = 7.50 Hz, Ar-H), 8.55 (d, 1H, *J* = 8.60 Hz, Ar-H), 8.61 (d, 1H, *J* = 5.80 Hz, Ar-H), 8.71 (s, 1H, CH=N), 8.91 (s, 1H, Ar-H, C3–H pyrazole), 11.68 (s, 1H, NH, exchanged with D_2O). ^{13}C NMR (DMSO, 100 MHz): 105.44, 119.54, 120.04, 121.21, 122.90, 123.14, 124.07, 125.09, 126.09, 127.44, 128.81, 129.72, 130.62, 131.66, 132.66, 133.57, 134.50, 135.09, 138.50, 145.96, 152.82, 154.90, 156.69. MS (*m/z*): 440 (M^+, 9.65%), 169 (100%). Anal. Calcd. for $C_{28}H_{20}N_6$ **(**440): C, 76.35; H, 4.58; N, 19.08. Found: C, 76.31; H, 4.55; N, 19.13.

5.1.3.11. *4-(2-(1-Phenylethylidene)hydrazinyl)- 1,6-Diphenyl-1H-pyrazolo[3,4-d] pyrimidine 15$_k$*

White solid; reaction time: 4 h yield 91% (0.37 g); m.p. 241 - 243°C. IR (KBr, *v*, cm^{-1}): 3202 (NH), 3075 (Ar-H), 2971 (aliph-CH). ^1H NMR (DMSO-d_6, 300 MHz): 2.96 (s, 3H, CH_3), 7.32 (t, 1H, *J* = 6.00 Hz, Ar-H), 7.35 (t, 1H, *J* = 9.00 Hz, Ar-H), 7.41 (t, 1H, *J* = 8.20 Hz, Ar-H), 7.54 (t, 2H, *J* = 6.00 Hz, Ar-H), 7.60 (t, 2H, *J* = 9.00 Hz, Ar-H), 7.97 (t, 2H, *J* = 8.20 Hz, Ar-H), 8.19 (d, 2H, *J* = 8.20 Hz, Ar-H), 8.34 (d, 2H, *J* = 5.90 Hz, Ar-H), 8.37 (d, 2H, *J* = 6.90 Hz, Ar-H), 8.58 (s, 1H, Ar-H, C3–H pyrazole), 11.17 (s, 1H, NH, exchanged with D_2O); ^{13}C NMR (DMSO, 100 MHz): 17.88, 102.63, 119.78, 120.82, 121.05, 123.44, 124.67, 125.20, 127.44, 128.83, 129.72, 131.67, 133.31, 135.09, 138.50, 149.99, 152.82, 154.90, 156.59. MS (*m/z*): 404 (M^+, 13.09%), 327 (100%); Anal. Calcd. for $C_{25}H_{20}N_6$ **(**404): C, 74.24; H, 4.98; N, 20.78. Found: C, 74.20; H, 4.94; N, 20.75.

5.1.3.12. *4-(2-(1-(4-Aminophenyl)ethylidene)hydrazinyl)-1,6-diphenyl-1H-pyrazolo[3,4-d]pyrimidine* **15$_l$**

White solid; reaction time was 4 h; yield 86% (0.36 g); m.p. 221 - 223°C; IR (KBr, *v*, cm^{-1}): 3320 - 3330 (NH_2), 3197 (NH), 3069 (Ar-H), 2968 (aliph-CH); ^1H NMR (DMSO-d_6, 300 MHz): 2.85 (s, 3H, CH_3), 5.49 (s, 2H, NH_2, exchanged with D_2O), 7.40 (d, 2H, *J* = 7.20 Hz, Ar-H), 7.58 (t, 1H, *J* =8.60 Hz, Ar-H), 7.61 (t, 1H, *J* = 6.80 Hz, Ar-H), 8.01 (t, 2H, *J* = 8.60 Hz, Ar-H), 8.13 (t, 2H, *J* = 6.80 Hz, Ar-H), 8.22 (d, 2H, *J* = 7.20 Hz, Ar-H), 8.23 (d, 2H, *J* = 5.40 Hz, Ar-H), 8.28 (d, 2H, *J* = 9.10 Hz, Ar-H), 8.58 (s, 1H, Ar-H, C3–H pyrazole), 11.36 (s, 1H, NH, exchanged with D_2O). ^{13}C NMR (DMSO, 100 MHz):

18.77, 103.32, 113.99, 121.03, 122.44, 123.88, 124.88, 125.04, 127.51, 129.75, 130.60, 132.55, 134.09, 138.50, 148.95, 150.14, 151.88, 153.98, 155.58. MS (*m/z*): 419 (M^+, 7.27%), 148 (100%). Anal. Calcd. for $C_{25}H_{21}N_7$ **(**419): C, 71.58; H, 5.05; N, 23.37. Found: C, 71.55; H, 5.02; N, 23.34.

5.1.3.13. *4-(2-(1-(p-Tolyl)ethylidene)hydrazinyl)-1,6-diphenyl-1H-pyrazolo[3,4-d] pyrimidine* 15_m

Yellowish white solid; reaction time: 3 h yield 84% (0.35 g); m.p.: 232 - 234°C; IR (KBr, *v*, cm^{-1}): 3191 (NH), 3087 (Ar-H), 2969 (aliph-CH). ^{1}H NMR (DMSO-d_6, 300 MHz): 2.49 (s, 3H, CH_3-ph), 2.99 (s, 3H, CH_3-imine) 7.24 (d, 2H, *J* = 5.70 Hz, Ar-H), 7.25 (t, 1H, *J* = 8.10 Hz, Ar-H), 7.30 (t, 1H, *J* = 7.50 Hz, Ar-H), 7.32 (t, 2H, *J* = 8.10 Hz, Ar-H), 7.57 (t, 2H, *J* = 7.50 Hz, Ar-H), 7.66 (d, 2H, *J* = 5.70 Hz, Ar-H), 8.10 (d, 2H, *J* = 6.10 Hz, Ar-H), 8.34 (d, 2H, *J* = 9.30 Hz, Ar-H), 8.58 (s, 1H, Ar-H, C3–H pyrazole), 11.69 (s, 1H, NH, exchanged with D_2O); ^{13}C NMR (DMSO, 100 MHz): 17.47, 22.78, 105.67, 120.87, 121.03, 123.44, 124.67, 125.20, 127.40, 128.83, 129.72, 131.67, 133.67, 135.09, 138.50, 141.78, 149.63, 151.89, 153.99, 155.59. MS (*m/z*): 418 (M^+, 15.49%), 91 (100%); Anal. Calcd. for $C_{26}H_{22}N_6$ **(**418): C, 74.62; H, 5.30; N, 20.08. Found: C, 74.66; H, 5.27; N, 20.04.

5.1.3.14. *4-(2-(1-(4-Fluorophenyl)ethylidene)hydrazinyl)-1,6-diphenyl-1H-pyrazolo[3,4-d] pyrimidine* 15_n

Green powder; reaction time: 4 h yield 80% (0.34 g); m.p.: 258 - 260°C; IR (KBr, *v*, cm^{-1}): 3213 (NH), 3089 (Ar-H), 2972 (aliph-CH). ^{1}H NMR (DMSO-d_6, 300 MHz): 2.50 (s, 3H, CH_3), 7.32 (d, 2H, *J* = 8.70 Hz, Ar-H), 7.35 (t, 1H, *J* =9.00 Hz, Ar-H), 7.41 (t, 1H, *J* =10.80 Hz, Ar-H), 7.60 (t, 2H, *J* = 9.00 Hz, Ar-H), 7.62 (t, 2H, *J* = 10.80 Hz, Ar-H), 7.99 (d, 2H, *J* = 8.70 Hz, Ar-H), 8.34 (d, 2H, *J* = 6.10 Hz, Ar-H), 8.37 (d, 2H, *J* = 7.30 Hz, Ar-H), 8.52 (s, 1H, Ar-H, C3–H pyrazole), 11.17 (s, 1H, NH, exchanged with D_2O). ^{13}C NMR (DMSO, 100 MHz): 17.14, 105.81, 121.03, 121.87, 123.44, 124.67, 125.20, 127.40, 128.03, 128.83, 130.67, 133.63, 135.12, 138.50, 149.63, 151.89, 153.41, 155.59, 157.57. MS (*m/z*): 422 (M^+, 18.25%), 151 (100%). Anal. Calcd. for $C_{25}H_{19}FN_6$ **(**422): C, 71.08; H, 4.53; N, 19.89. Found: C, 71.13; H, 4.57; N, 19.86.

5.1.3.15. *4-(2-(1-(4-Bromophenyl)ethylidene)hydrazinyl)-1,6-diphenyl-1H-pyrazolo[3,4-d]pyrimidine* 15_o

Orange crystal; reaction time: 8 h yield 77% (0.37 g); m.p. 267 - 269°C; IR (KBr, *v*, cm^{-1}): 3218 (NH), 3085 (Ar-H), 2972 (aliph-CH). ^{1}H NMR (DMSO-d_6, 300 MHz): 2.95 (s, 3H, CH_3), 7.33 (t, 1H, *J* = 7.80 Hz, Ar-H), 7.41 (t, 1H, *J* = 6.90 Hz, Ar-H), 7.46 (t, 2H, *J* = 7.80 Hz, Ar-H), 7.52 (t, 2H, *J* = 6.90 Hz, Ar-H), 7.57 (d, 2H, *J* = 8.10 Hz, Ar-H), 8.14 (d, 2H, *J* = 8.10 Hz, Ar-H), 8.35 (d, 2H, *J* = 6.30 Hz, Ar-H), 8.57 (d, 2H, *J* = 8.30 Hz, Ar-H), 8.61 (s, 1H, Ar-H, C3–H pyrazole), 11.26 (s, 1H, NH, exchanged with D_2O). ^{13}C NMR (DMSO, 100 MHz): 17.78, 106.66, 115.77, 121.03, 122.44, 124.07, 124.67, 127.04, 127.81, 129.72, 130.67, 132.67, 134.09, 137.50, 148.93, 151.88, 153.98, 155.58, 158.14. MS (*m/z*): 484 (M^++2, 8.55%), 482 (M^+, 8.51%), 210 (100%). Anal. Calcd. for $C_{25}H_{19}BrN_6$ **(**482): C, 62.12; H, 3.96; N, 17.39. Found: C, 62.14; H, 3.99; N, 17.42.

5.1.4. 4-(2-(Indolin-2-on-3-yl)hydrazinyl)-1,6-diphenyl-1H-pyrazolo[3,4-d] pyrimidine 16

To a solution of **14** (0.3, 0.001 mol) in glacial acetic acid (20 mL), isatin (0.14 g, 0.001 mol) was added. Then, the mixture was heated under reflux for 24 h. The reaction mixture was concentrated and allowed to cool. The separated solid was filtered and recrystallized from glacial acetic acid to give the target compound **16**.

Orange crystal (0.32 g, 74%); m.p. 271- 273 °C; IR (KBr, *v*, cm^{-1}): 3225 (NH), 3076 (Ar-H), 1715 (C=O). ^{1}H NMR (DMSO-d_6, 300 MHz): 7.40 (t, 1H, *J* =7.50 Hz, Ar-H), 7.54 (t, 1H, *J* = 5.40 Hz, Ar-H), 7.57 (t, 1H, *J* = 12.00 Hz, Ar-H), 7.62 (t, 2H, *J* = 5.40 Hz, Ar-H), 7.67 (t, 2H, *J* = 12.00 Hz, Ar-H), 8.27 (t, 1H, *J* =7.50 Hz, Ar-H), 8.30 (d, 1H, *J* = 9.50 Hz, Ar-H), 8.41 (d, 1H, *J* = 8.80 Hz, Ar-H), 8.43 (d, 2H, *J* = 8.40 Hz, Ar-H), 8.44 (d, 2H, *J* =7.90 Hz, Ar-H), 8.59 (s, 1H, Ar-H, C3–H pyrazole), 11.35 (s, 1H, NH, exchanged with D_2O imine), 13.29 (s, 1H, NH exchanged with D_2O). ^{13}C NMR (DMSO, 100 MHz): 102.31, 116.51, 119.54, 120.04, 122.94, 124.07, 125.09, 127.44, 128.81, 129.66, 129.72, 133.06, 133.57, 135.09, 138.50, 140.69, 145.92, 152.89, 154.96, 156.56, 159.61. MS (*m/z*): 431 (M^+, 22.51%), 160 (100%). Anal. Calcd. for $C_{25}H_{17}N_7O$ **(**431): C, 69.60; H, 3.97; N, 22.72. Found: C, 69.65; H, 3.93; N, 22.68.

5.1.5. General procedure for preparation of compounds17$_{a-f}$

To a solution of compound **14** (0.3, 0.001 mol) in butanol (20 ml), appropriate isocyanates or isothiocyanates (0.001 mol) namely, ethyl isothiocyanates, ethyl isocyanates, cyclohexyl isothiocyanates, cyclohexyl isocyanates, phenyl isothiocyanates, and/or phenyl isocyanates was added drop wise at 0^{o}C. The mixture was stirred for specific time at room temperature. Then, the solvent was evaporated under reduced pressure and crude product was purified by crystallization from methanol to yield the corresponding compounds **17$_{a-f}$**, respectively .

5.1.5.1. 2-(1,6-Diphenyl-1H-pyrazolo[3,4-d]pyrimidin-4-yl)-N-ethylhydrazine-1-carbothioamide 17$_a$

Grayish-white solid; reaction time: 8 h; yield 74% (0.29 g); m.p. 280 - 282°C; IR (KBr, *v*, cm^{-1}): 3320 (NH), 3080 (Ar-H), 2970 (aliph-CH); ^{1}H NMR (DMSO-d_6, 300 MHz): 1.17 (t, 3H, *J* = 6.9 Hz, -$CH_2C\underline{\mathbf{H}}_3$), 4.16 (q, 2H, *J* = 7.2 Hz, -$C\underline{\mathbf{H}}_2CH_3$), 7.40 (t, 1H, *J* = 7.50 Hz, Ar-H), 7.54 (t, 1H, *J* =10.50 Hz, Ar-H), 7.62 (t, 2H, *J* = 7.50 Hz, Ar-H), 7.67 (t, 2H, *J* = 10.50 Hz, Ar-H), 8.29 (d, 2H, *J* = 9.80 Hz, Ar-H), 8.59 (d, 2H, *J* = 6.20 Hz, Ar-H), 8. 69 (s, 1H, Ar-H, C3–H pyrazole), 9.77 (s, 1H, NH exchanged with D_2O), 10.51 (s, 1H, NH exchanged with D_2O), 12.09 (s, 1H, NH exchanged with D_2O); ^{13}C NMR (DMSO, 100 MHz): 15.91, 42.41, 102.19, 120.54, 121.14, 124.44, 125.66, 128.96, 129.31, 133.45, 135.27, 138.51, 152.82, 154.90, 156.59, 179.52; MS (*m/z*): 389 (M^+, 15.14%), 271 (100%). Anal. Calcd. for $C_{20}H_{19}N_7S$ **(**389): C, 61.68; H, 4.92; N, 25.17. Found: C, 61.65; H, 4.94; N, 25.12.

5.1.5.2.2-(1,6-Diphenyl-1H-pyrazolo[3,4-d]pyrimidin-4-yl)-N-ethylhydrazine-1-carboxamide 17$_b$

Brownish solid; reaction time: 6 h; yield 78% (0.29 g); m.p. 274 - 276°C; IR (KBr, *v*, cm^{-1}): 3335 (NH), 3084 (Ar-H), 2970 (aliph-CH), 1666 (C=O); ^{1}H NMR (DMSO-d_6, 300 MHz): 1.16 (t, 3H, *J* = 7.2 Hz, -$CH_2C\underline{\mathbf{H}}_3$), 4.05 (q, 2H, *J* = 7.2 Hz, -$C\underline{\mathbf{H}}_2CH_3$), 7.38 (t, 1H, *J* = 7.80 Hz, Ar-H), 7.57 (t, 1H, *J* =7.50 Hz, Ar-H), 7.62 (t, 2H, *J* = 7.80 Hz, Ar-H), 8.13 (t, 2H, *J* = 7.50 Hz, Ar-H), 8.26 (d, 2H, *J* = 5.70 Hz, Ar-H), 8.55 (d, 2H, *J* = 9.20 Hz, Ar-H), 8. 63 (s, 1H, Ar-H, C3–H pyrazole), 9.50 (s, 1H, NH exchanged with D_2O),

10.14 (s, 1H, NH exchanged with D_2O), 11.92 (s, 1H, NH exchanged with D_2O); ^{13}C NMR (DMSO, 100 MHz): 14.62, 35.91, 105.16, 120.28, 121.56, 124.98, 125.32, 128.90, 129.20, 133.24, 135.99, 138.61, 152.07, 154.94, 156.51, 169.16; MS (*m/z*): 373 (M^+, 15.14%), 102 (100%). Anal. Calcd. for $C_{20}H_{19}N_7O$ **(**373): C, 64.33; H, 5.13; N, 26.26. Found: C, 64.36; H, 5.16; N, 26.29.

5.1.5.3. N-cyclohexyl-2-(1,6-diphenyl-1H-pyrazolo[3,4-d]pyrimidin-4-yl)hydrazine-1-carbothioamide 17$_c$

White solid; reaction time: 9 h; yield 70% (0.31 g); m.p. 265 - 267°C; IR (KBr, *v*, cm^{-1}): 3313 (NH), 3089 (Ar-H), 2976 (aliph-CH); ^1H NMR (DMSO-d_6, 300 MHz): 1.63 - 2.18 (m, 10H, Cyclohexyl), 3.78 (m, 1H, -NHC**H**-Cyclohexyl), 7.38 (t, 1H, *J* = 8.40 Hz, Ar-H), 7.57 (t, 1H, *J* = 7.50 Hz, Ar-H), 7.66 (t, 2H, *J* = 8.40 Hz, Ar-H), 8.13 (t, 2H, *J* = 7.50 Hz, Ar-H), 8.35 (d, 2H, *J* = 5.80 Hz, Ar-H), 8.48 (d, 2H, *J* = 9.20 Hz, Ar-H), 8. 69 (s, 1H, Ar-H, C3–H pyrazole), 9.80 (s, 1H, NH exchanged with D_2O), 10.81 (s, 1H, NH exchanged with D_2O), 11.93 (s, 1H, NH exchanged with D_2O); ^{13}C NMR (DMSO, 100 MHz): 25.21, 25.67, 33.45, 35.27, 104.99, 121.76, 124.07, 124.44, 125.35, 128.24, 129.29, 133.47, 135.23, 138.51, 152.82, 154.90, 156.59, 180.10; MS (*m/z*): 443 (M^+, 12.12%), 172 (100%). Anal. Calcd. for $C_{24}H_{25}N_7S$ **(**443): C, 64.99; H, 5.68; N, 22.10. Found: C, 64.95; H, 5.65; N, 22.14.

5.1.5.4. N-cyclohexyl-2-(1,6-diphenyl-1H-pyrazolo[3,4-d]pyrimidin-4-yl)hydrazine-1-carboxamide 17$_d$

White solid; reaction time: 7 h; yield 68% (0.29 g); m.p. 255 - 257°C. IR (KBr, *v*, cm^{-1}): 3318 (NH), 3091 (Ar-H), 2976 (aliph-CH), 1678 (C=O); ^1H NMR (DMSO-d_6, 300 MHz): 1.14 - 1.75 (m, 10H, Cyclohexyl), 3.56 (m, 1H, -NHC**H**-Cyclohexyl), 7.41 (t, 1H, *J* = 7.20 Hz, Ar-H), 7.59 (t, 1H, *J* =8.10 Hz, Ar-H), 7.67 (t, 2H, *J* = 7.20 Hz, Ar-H), 8.32 (t, 2H, *J* = 8.10 Hz, Ar-H), 8.46 (d, 2H, *J* = 10.80 Hz, Ar-H), 8.52 (d, 2H, *J* = 6.20 Hz, Ar-H), 8. 74 (s, 1H, Ar-H, C3–H pyrazole), 9.67 (s, 1H, NH exchanged with D_2O), 10.70 (s, 1H, NH exchanged with D_2O), 11. 81 (s, 1H, NH exchanged with D_2O); ^{13}C NMR (DMSO, 100 MHz): 13.49, 15.67, 30.45, 31.73, 104.80, 121.13, 122.71, 123.14, 126.77, 128.87, 129.60, 132.58, 136.51, 139.51, 152.73, 154.24, 156.27, 170.15; MS m/z (%):

427 (M^+, 22.12%), 330 (100%). Anal. Calcd. for $C_{24}H_{25}N_7O$ **(**427): C, 67.43; H, 5.89; N, 22.93. Found: C, 67.45; H, 5.85; N, 22.91.

5.1.5.5. *2-(1,6-Diphenyl-1H-pyrazolo[3,4-d]pyrimidin-4-yl)-N-phenylhydrazine-1-carbothioamide* 17_e

Green crystal; reaction time: 15 h; yield 64% (0.28 g); m.p. 295 - 297°C; IR (KBr, *v*, cm^{-1}): 3324 (NH), 3067 (Ar-H); ^{1}H NMR (DMSO-d_6, 300 MHz): 7.10 (t, 1H, *J* = 6.90 Hz, Ar-H), 7.21 (t, 2H, *J* =6.90 Hz, Ar-H), 7.54 (t, 1H, *J* =7.80 Hz, Ar-H), 7.65 (t, 1H, *J* =8.40 Hz, Ar-H), 7.67 (t, 2H, *J* = 7.80 Hz, Ar-H), 8.28 (t, 2H, *J* = 8.40 Hz, Ar-H), 8.31 (d, 2H, *J* = 9.30 Hz, Ar-H), 8.48 (d, 2H, *J* = 10.20 Hz, Ar-H), 8.50 (d, 2H, *J* = 11.80 Hz, Ar-H), 8.61 (s, 1H, Ar-H, C3–H pyrazole), 10.23 (s, 1H, NH, exchanged with D_2O), 11.38 (s, 1H, NH, exchanged with D_2O), 12.60 (s, 1H, NH, exchanged with D_2O); ^{13}C NMR (DMSO, 100 MHz): 102.87, 121.13, 122.71, 123.14, 124.44, 125.35, 126.74, 127.44, 128.81, 129.72, 131.24, 133.27, 136.49, 138.50, 152.92, 153.22, 154.59, 181.90. MS (*m/z*): 437 (M^+, 15.84%), 166 (100.00). Anal. Calcd. for $C_{24}H_{19}N_7S$ **(**437): C, 65.89; H, 4.38; N, 22.41. Found: C, 65.85; H, 4.34; N, 22.45.

5.1.5.6. *2-(1,6-Diphenyl-1H-pyrazolo[3,4-d]pyrimidin-4-yl)-N-phenylhydrazine-1-carboxamide* 17_f

Orange needle; reaction time: 13 h yield 71% (0.30 g); m.p. 285 - 287°C; IR (KBr, *v*, cm^{-1}): 3309 (NH), 3059 (Ar-H), 1675 (C=O); ^{1}H NMR (DMSO-d_6, 300 MHz): 7.24 (t, 1H, *J* = 5.40 Hz, Ar-H), 7.25 (t, 2H, *J* = 8.10 Hz, Ar-H), 7.32 (d, 2H, *J* = 5.40 Hz, Ar-H), 7.35 (t, 1H, *J* = 6.60 Hz, Ar-H), 7.63 (t, 1H, *J* = 8.10 Hz, Ar-H), 7.71 (t, 2H, *J* = 7.80 Hz, Ar-H), 8.14 (t, 2H, *J* = 10.10 Hz, Ar-H), 8.38 (d, 2H, *J* = 6.60 Hz, Ar-H), 8.50 (d, 2H, *J* = 8.10 Hz, Ar-H), 8.63 (s, 1H, Ar-H, C3–H pyrazole), 9.57 (s, 1H, NH, exchanged with D_2O), 10.39 (s, 1H, NH, exchanged with D_2O), 11.69 (s, 1H, NH, exchanged with D_2O); ^{13}C NMR (DMSO, 100 MHz): 102.70, 121.13, 121.71, 123.14, 123.44, 127.09, 127.44, 127.74, 128.72, 129.81, 130.24, 133.49, 136.27, 139.50, 151.92, 153.59, 154.22, 171.59. MS (*m/z*): 421 (M^+, 14.37%), 301 (100%). Anal. Calcd. for $C_{24}H_{19}N_7O$ **(**421): C, 68.40; H, 4.54; N, 23.26. Found: C, 68.405; H, 4.49; N, 23.22,

5.1.6. General procedure for preparation of compounds18$_{a-e}$

A solution of compound **14** (0.3, 0.001 mol) and the appropriate benzoyl chloride derivatives (0.001 mol) namely, benzoyl chloride, 4-methoxybenzoyl chloride, 4-methyl benzoyl chloride, 4-fluorobenzoyl chloride and 4-chlorobenzoyl chloride in DMF (20 ml) in presence of catalytic amount of TEA (0.5 ml) was stirred at room temperature for specific time then poured onto ice-cold water. The obtained precipitate was filtered, washed with water, dried and crystallized from glacial acetic acid to afford compounds **18_{a-e}**, respectively.

5.1.6.1. N'-(1,6-diphenyl-1H-pyrazolo[3,4-d]pyrimidin-4-yl)benzohydrazide 18_a

White solid; reaction time: 3 h; yield 69% (0.28 g); m.p. 256 - 258°C; IR (KBr, *v*, cm^{-1}): 3320 (NH), 3091 (Ar-H), 1681 (C=O); ^{1}H NMR (DMSO-d_6, 300 MHz): 7.32 (t, 1H, *J* = 8.70 Hz, Ar-H), 7.35 (t, 1H, *J* = 9.30 Hz, Ar-H), 7.38 (t, 2H, *J* =8.10 Hz, Ar-H), 7.60 (t, 2H, *J* = 8.70 Hz, Ar-H), 7.65 (t, 2H, *J* = 9.30 Hz, Ar-H), 7.95 (t, 1H, *J* = 8.10 Hz, Ar-H), 7.99 (d, 2H, *J* = 6.30 Hz, Ar-H), 8.34 (d, 2H, *J* = 6.20 Hz, Ar-H), 8.37 (d, 2H, *J* = 6.80 Hz, Ar-H), 8.52 (s, 1H, Ar-H, C3–H pyrazole), 11.17 (s, 1H, NH, exchanged with D_2O), 11.96 (s, 1H, NH, exchanged with D_2O); ^{13}C NMR (DMSO, 100 MHz): 106.47, 120.54, 121.21, 122.14, 124.70, 125.00, 127.23, 128.18, 129.54, 130.60, 131.66, 132.57, 135.02, 138.52, 152.82, 154.90, 156.59, 170.09. MS (*m/z*): 406 (M^+, 5.29%), 77 (100%). Anal. Calcd. for $C_{24}H_{18}N_6O$ **(**406): C, 70.92; H, 4.46; N, 20.68. Found: C, 70.96; H, 4.49; N, 20.63.

5.1.6.2. N'-(1,6-Diphenyl-1H-pyrazolo[3,4-d]pyrimidin-4-yl)-4-methoxybenzohydrazide 18_b

White solid; reaction time: 4 h yield 76% (0.33 g); m.p. 262 - 264°C; IR (KBr, *v*, cm^{-1}): 3339 (NH), 3094 (Ar-H), 2980 (aliph-CH), 1688 (C=O); ^{1}H NMR (DMSO-d_6, 300 MHz): 3.95 (s, 3H, OCH_3), 7.33 (d, 2H, *J* = 8.10 Hz, Ar-H), 7.41 (t, 1H, *J* =6.90 Hz, Ar-H), 7.46 (t, 1H, *J* = 12.00 Hz, Ar-H), 7.50 (t, 2H, *J* = 6.90 Hz, Ar-H), 7.57 (t, 2H, *J* = 12.00 Hz, Ar-H), 8.17 (d, 2H, *J* = 8.10 Hz, Ar-H), 8.35 (d, 2H, *J* = 9.80 Hz, Ar-H), 8.57 (d, 2H, *J* = 7.10 Hz, Ar-H), 8.61 (s, 1H, Ar-H, C3–H pyrazole), 10.26 (s, 1H, NH, exchanged with D_2O), 11.62 (s, 1H, NH, exchanged with D_2O); ^{13}C NMR (DMSO, 100 MHz): 56.59, 106.96, 115.82, 121.28, 122.44, 127.05, 128.61, 128.81, 128.91, 129.44,

129. 61, 132.73, 135.09, 138.91, 152.82, 154.91, 156.59, 161.45, 170.09. MS (*m/z*): 436 (M^+, 8.46%), 165 (100%). Anal. Calcd. for $C_{25}H_{20}N_6O_2$ **(**436): C, 68.80; H, 4.62; N, 19.25. Found: C, 68.85; H, 4.67; N, 19.20.

5.1.6.3. N'-(1,6-diphenyl-1H-pyrazolo[3,4-d]pyrimidin-4-yl)-4-methylbenzohydrazide 18$_c$

White solid; reaction time: 4 h yield 74% (0.31 g); m.p. 245 - 247°C; IR (KBr, *v*, cm^{-1}): 3341 (NH), 3062 (Ar-H), 2989 (aliph-CH), 1672 (C=O); ^{1}H NMR (DMSO-d_6, 300 MHz): 2.50 (s, 3H, CH_3), 7.40 (d, 2H, *J* = 7.50 Hz, Ar-H), 7.56 (t, 1H, *J* =5.70 Hz, Ar-H), 7.60 (t, 1H, *J* = 8.40 Hz, Ar-H), 7.62 (t, 2H, *J* = 5.70 Hz, Ar-H), 7.65 (t, 2H, *J* = 8.40 Hz, Ar-H), 8.30 (d, 2H, *J* = 7.50 Hz, Ar-H), 8.44 (d, 2H, *J* = 9.80 Hz, Ar-H), 8.49 (d, 2H, *J* = 6.10 Hz, Ar-H), 8.59 (s, 1H, Ar-H, C3–H pyrazole), 10.41 (s, 1H, NH, exchanged with D_2O), 11.44 (s, 1H, NH, exchanged with D_2O); ^{13}C NMR (DMSO, 100 MHz): 21.01, 102.36, 121.11, 121.33, 123.16, 124.70, 125.09, 127.41, 128.84, 129.76, 131.62, 133.55, 135.05, 138.59, 140.70, 152.20, 154.68, 156.04, 170.04. MS (*m/z*): 420 (M^+, 6.18%), 286 (100%). Anal. Calcd. for $C_{25}H_{20}N_6O$ **(**420): C, 71.41; H, 4.79; N, 19.99. Found: C, 71.44; H, 4.75; N, 19.93.

5.1.6.4.N'-(1,6-diphenyl-1H-pyrazolo[3,4-d]pyrimidin-4-yl)-4-fluorobenzohydrazide 18$_d$

Orange crystal; reaction time: 3 h yield 75% (0.32 g); m.p. 306 - 308°C; IR (KBr, *v*, cm^{-1}): 3334 (NH), 3091 (Ar-H), 1684 (C=O); ^{1}H NMR (DMSO-d_6, 300 MHz): 7.40 (d, 2H, *J* = 7.50 Hz, Ar-H), 7.43 (t, 1H, *J* = 7.50 Hz, Ar-H), 7.55 (t, 1H, *J* = 6.00 Hz, Ar-H), 7.67 (t, 2H, *J* = 7.50 Hz, Ar-H), 8.29 (t, 2H, *J* = 6.00 Hz, Ar-H), 8.41 (d, 2H, *J* = 7.50 Hz, Ar-H), 8.43 (d, 2H, *J* = 10.80 Hz, Ar-H), 8.44 (d, 2H, *J* = 9.10 Hz, Ar-H), 8.59 (s, 1H, Ar-H, C3–H pyrazole), 10.39 (s, 1H, NH, exchanged with D_2O), 11.38 (s, 1H, NH, exchanged with D_2O); ^{13}C NMR (DMSO, 100 MHz): 106.47, 123.14, 123.81, 125.00, 125.70, 128.18, 128.52, 130.06, 130.30, 131.66, 133.57, 136.02, 137.52, 152.62, 154.10, 156.30, 158.92, 171.82. MS (*m/z*): 424 (M^+, 13.65%), 153 (100%). Anal. Calcd. for $C_{24}H_{17}FN_6O$ **(**424): C, 67.92; H, 4.04; N, 19.80. Found: C, 67.72; H, 4.14; N, 19.65.

5.1.6.5. 4-Chloro-N'-(1,6-diphenyl-1H-pyrazolo[3,4-d]pyrimidin-4-yl)benzohydrazide 18$_e$

Brown solid; reaction time: 7 h yield 66% (0.29 g); m.p. 281 - 282°C; IR (KBr, *v*, cm^{-1}): 3345 (NH), 3082 (Ar-H), 1678 (C=O); ^{1}H NMR (DMSO-d_6, 300 MHz): 7.10 (t, 1H, *J* = 6.90 Hz, Ar-H), 7.21 (t, 1H, *J* = 7.80 Hz, Ar-H), 7.43 (d, 2H, *J* = 7.20 Hz, Ar-H), 7.55 (t, 2H, *J* = 6.90 Hz, Ar-H), 7.68 (t, 2H, *J* = 7.80 Hz, Ar-H), 8.29 (d, 2H, *J* = 7.20 Hz, Ar-H), 8.32 (d, 2H, *J* = 10.80 Hz, Ar-H), 8.48 (d, 2H, *J* = 9.10 Hz, Ar-H), 8.60 (s, 1H, Ar-H, C3–H pyrazole), 9.88 (s, 1H, NH, exchanged with D_2O), 10.84 (s, 1H, NH, exchanged with D_2O); ^{13}C NMR (DMSO, 100 MHz): 106.48, 123.21, 127.07, 127.18, 127.57, 129.21, 129.68, 129.74, 130.18, 131.29, 132.51, 135.12, 138.22, 152.88, 154.98, 156.58, 157.12, 171.52. MS (*m/z*): 440 (M^+, 9.18%), 169 (100%). Anal. Calcd. for $C_{24}H_{17}ClN_6O$ **(**440): C, 65.38; H, 3.89; N, 19.06. Found: C, 65.33; H, 3.84; N, N, 19.11.

5.1.7. 2-((1,6-Diphenyl-1H-pyrazolo[3,4-d]pyrimidin-4-yl)amino)isoindoline-1,3-dione 19

To a solution of **14** (0.3, 0.001 mol) in glacial acetic acid (20 mL), phthalic anhydride (0.15 g, 0.001 mol) was added. The mixture was heated under reflux for 16 h. After completion of the reaction mixture, it was concentrated and allowed to cool. The separated solid was filtered and crystallized from methanol to produce the target compound **19**.

Blue solid; yield72% (0.31 g), m.p. 279 - 281 °C; IR (KBr, *v*, cm^{-1}): 3218 (NH), 3079 (Ar-H), 1713 (2C=O). ^{1}H NMR (DMSO-d_6, 300 MHz): 7.28 (t, 1H, *J* =6.90 Hz, Ar-H), 7.41 (t, 1H, *J* = 9.00 Hz, Ar-H), 7.61 (t, 2H, *J* = 6.90 Hz, Ar-H), 7.99 (t, 2H, *J* = 9.00 Hz, Ar-H), 8.13 (d, 2H, *J* = 7.20 Hz, Ar-H), 8.25 (d, 2H, *J* = 7.20 Hz, Ar-H), 8.46 (d, 2H, *J* = 10.30 Hz, Ar-H), 8.58 (d, 2H, *J* = 7.10 Hz, Ar-H), 8.85 (s, 1H, Ar-H, C3–H pyrazole), 11.36 (s, 1H, NH, exchanged with D_2O); ^{13}C NMR (DMSO, 100 MHz): 102.13, 121.21, 123.14, 124.12, 125.09, 127.04, 128.72, 129.81, 131.56, 132.66, 135.57, 137.09, 139.50, 152.12, 154.10, 156.56, 158.15. MS (*m/z*): 432 (M^+, 9.51%), 286 (100%). Anal. Calcd. for $C_{25}H_{16}N_6O_2$ **(**432): C, 69.44; H, 3.73; N, 19.43. Found: C, 69.40; H, 3.78; N, 19.48.

5.1.8. 4-(3,5-Dimethyl-1H-pyrazol-1-yl)-1,6-diphenyl-1H-pyrazolo[3,4-d]pyrimidine 20

A mixture of compound **14** (0.3, 0.001 mol) and acetyl acetone (0.1 g, 0.01 mol) in glacial acetic acid (20 mL) was heated under reflux for 48 h. Then, the reaction mixture was poured onto crushed ice with continuous stirring and filtered. The obtained solid was crystallized from ethanol to yield the targeted compound **20.**

White solid; yield 66% (0.24 g); m.p. 244 - 246°C; IR (KBr, *v*, cm^{-1}): 3069 (Ar-H), 2985 (aliph-CH). ^{1}H NMR (DMSO-d_6, 300 MHz): 2.50 (s, 3H, -CH_3), 2.80 (s, 3H, CH_3), 6.25 (s, 1H, free pyrazole), 7.40 (t, 1H, *J* = 7.20 Hz, Ar-H), 7.58 (t, 1H, *J* =7.50 Hz, Ar-H), 7.60 (t, 2H, *J* = 10.50 Hz, Ar-H), 8.19 (t, 2H, *J* = 9.40 Hz, Ar-H), 8.21 (d, 2H, *J* = 7.20 Hz, Ar-H), 8.37 (d, 2H, *J* = 7.50 Hz, Ar-H), 8.67 (s, 1H, Ar-H, C3–H pyrazole); ^{13}C NMR (DMSO, 100 MHz): 13.24, 14.48, 104.78, 109.78, 124.07, 125.21, 126.11, 127.41, 128.13, 129.79, 133.09, 135.57, 138.50, 140.96, 150.66, 152.82, 154.90, 156.59. MS (*m/z*): 366 (M^+, 18.18%), 271(100%). Anal. Calcd. for $C_{22}H_{18}N_6$ **(**366): C, 72.11; H, 4.95; N, 22.94. Found: C, 72.16; H, 4.99; N, 22.97.

5.2. Biological evaluation

5.2.1. $EGFR^{WT}$ and $EGFR^{T790M}$ kinase inhibitory assay

The *in vitro* inhibitory activities of the synthesized compounds against $EGFR^{WT}$ and $EGFR^{T790M}$ were carried out using homogeneous time resolved fluorescence (HTRF) assay [59]. $EGFR^{WT}$, $EGFR^{T790M}$ and ATP were purchased from Sigma. At first, the $EGFR^{WT}$ and/or $EGFR^{T790M}$ and their substrates were incubated with the synthesized compounds in enzymatic buffer for 5 min. in order to start the enzymatic reaction, ATP (1.65 µM) was added into the reaction mixture. The assay were conducted for 30 min at room temperature. The reaction was stopped by addition of detection reagents which contain EDTA. The detection step continued for 1 h, then the IC_{50} values were

determined by GraphPad Prism 5.0. Three independent experiments were performed for each concentration.

5.2.2. *In vitro* anti-proliferative activities

Thirteen compounds (**15_b, 15_e, 15_g, 15_i, 15_h, 15_n, 15_o, 17_a, 17_b, 17_d, 17_f, 18_d** and **18_e)** that exhibited promising IC_{50} values against EGFR-TK were tested for their anti-proliferative activities against three types of human cancer cell lines (breast adenocarcinoma MCF-7, hepatocellular carcinoma (HepG2), and non-small cell lung cancer cells (A549, H1975 and HCC827). four commercially available drugs (lapatinib, sorafinib, erlotinib and osimertinib) were used as positive controls.

Anti-proliferative activities of the synthesized compounds were carried out based on MTT assay [60]. Briefly, human cancer cell lines were dropped in 96-well plates at a density of 3-8 × 10^3 cells/well. Next, the wells were incubated for 12 h in a 5% CO2 incubator at 37 °C. Then, for each well, the growth medium was exchanged with 0.1 ml of fresh medium containing graded concentrations of the test compounds to be or equal DMSO and incubated for two days. Then 10 µl MTT solution (5 µg/ml) was added to each well, and the cells were incubated for additional 4 h. The crystals of MTT-formazan were dissolved in 100 µl of DMSO; the absorbance of each well was measured at 490 nm using an automatic ELISA reader system (TECAN, CHE). The IC_{50} values were calculated using the nonlinear regression fitting models (Graph Pad, Prism Version 5). The means of at least three separate experiments gave the reported results. Statistical differences were analyzed according to one way ANOVA test wherein the differences were considered to be significant at $p < 0.05$.

5.2.3. *In-vitro* DNA-Flow cytometric (cell cycle) analysis.

HepG2 cells were exposed to the most active member **18_d** for 24 h. Then, the tested cells were collected by trypsinization and washed in PBS. Ice-cold absolute ethanol was used for fixation of the collected cells. The cells were stained with Cycle TESTTM PLUS DNA Reagent Kit (BD Biosciences, San Jose, CA) according to the manufacturer's instructions. Cell-cycle distribution was evaluated using a flow cytometer.

5.2.4. Annexin V-FITC apoptosis assay.

As described above, HepG2 cells were seeded and incubated with compound **18_d** for 24 h. Then, the cells were collected and washed with PBS two successive times. The cells were exposed to centrifugation. Thereafter, the cells were treated with Annexin V-FITC and propidium iodide (PI) using the apoptosis detection kit (BD Biosciences, San Jose, CA) according to the manufacturer's protocol. Annexin V-FITC and PI binding were analyzed by a flow cytometer.

5.3. Molecular modeling

5.3.1. Docking studies

Crystallographic structures of $EGFR^{WT}$ and $EGFR^{T790M}$ were retrieved from Protein Data Bank [PDB ID: 4HJO, resolution 2.75 Å and PDB ID: 3W2O, resolution 2.35 Å, respectively] (http://www.pdb.org), and considered as targets for docking simulations. The docking analysis was performed using MOE [70] software to evaluate the free energies and binding mode of the designed molecules against $EGFR^{WT}$ and $EGFR^{T790M}$. At first, the crystal structures of $EGFR^{WT}$ and $EGFR^{T790M}$ were prepared by removing water molecules and retaining only one chain and their co-crystallized ligands, erlotinib and TAK-285, respectively. Then, the protein structures were protonated and the hydrogen atoms were hided. Next, the energy was minimized and the binding pockets of the protein were defined.

The 2D structures of the synthesized compounds and the co-crystallized ligands, erlotinib and TAK-285 were sketched using ChemBioDraw Ultra 14.0 and saved as MDL-SD format. Then, the saved files were opened using MOE and 3D structures were protonated. Next, energy minimization was applied. Before docking the synthesized compounds, validation of the docking protocol was carried out by running the simulation only using the co-crystallized ligands and low RMSD between docked and crystal conformations. The molecular docking of the synthesized compounds and the co-crystallized ligands was performed using a default protocol. In each case, 30 docked structures were generated using genetic algorithm searches. The output from of MOE was further analyzed and visualized using Discovery Studio 2.5 software.

Appendix A. Supplementary data

Supplementary data related to this manuscript is found in separated file.

Conflict of interest

None

Acknowledgement

Authors are thankful to the scientific research team of Regional Center of Mycology and Biotechnology, Faculty of Science, Al-Azhar University, Cairo, Egypt, as well as the biologists of VACSERA CO., Giza, Egypt for providing laboratory facilities for biological testing.

Appendix A. Supplementary data

Supplementary data related to this manuscript is found in separated file.

References

1) L.A. Torre, F. Bray, R.L. Siegel, J. Ferlay, J. Lortet-Tieulent, A. Jemal, Global cancer statistics, 2012, CA: A Cancer J. Clin. 65 (2) (2015) 87-108.
2) G.L. Patrick, An introduction to medicinal chemistry, 5th edition,Oxford university press (2013) 515-524.
3) J. Chang, H. Ren, M. Zhao, Y. Chong, W. Zhao, Y. He, Y. Zhao, H. Zhang, C. Qi, Development of a series of novel 4-anlinoquinazoline derivatives possessing quinazoline skeleton: Design, synthesis, EGFR kinase inhibitory efficacy, and evaluation of anticancer activities in vitro, Eur. J. Med. Chem. 138 (2017) 669-688.
4) V.S. Kasture, D.S. Musmade, S.J. Aher, P.P. Patil, Tyrosine Kinases: promising targets for cancer chemotherapy, Med. Chem. Drug Discov. 2 (2) (2012) 37-51.
5) M. Huang, A. Shen, J. Ding, M. Geng, Molecularly targeted cancer therapy: some lessons from the past decade, Trends Pharmacol. Sci. 35 (1) (2014) 41-50.
6) J.D. Clark, M.E. Flanagan, J.-B. Telliez, Discovery and Development of Janus Kinase (JAK) Inhibitors for Inflammatory Diseases: Miniperspective, J. Med. Chem. 57 (12) (2014) 5023-5038.
7) F. Muth, M. Günther, S.M. Bauer, E. Döring, S. Fischer, J. Maier, P. Drückes, J.r. Köppler, J.r. Trappe, U. Rothbauer, Tetra-substituted pyridinylimidazoles as dual inhibitors of p38α mitogen-activated protein kinase and c-Jun N-terminal kinase 3

for potential treatment of neurodegenerative diseases, J. Med. Chem. 58 (1) (2014) 443-456.

8) R. Kikuchi, K. Nakamura, S. MacLauchlan, D.T.-M. Ngo, I. Shimizu, J.J. Fuster, Y. Katanasaka, S. Yoshida, Y. Qiu, T.P. Yamaguchi, An antiangiogenic isoform of VEGF-A contributes to impaired vascularization in peripheral artery disease, Nature Medicine 20 (12) (2014) 1464-1471.
9) A.S. Banks, F.E. McAllister, J.P.G. Camporez, P.-J.H. Zushin, M.J. Jurczak, D. Laznik-Bogoslavski, G.I. Shulman, S.P. Gygi, B.M. Spiegelman, An ERK/Cdk5 axis controls the diabetogenic actions of PPARγ, Nature 517 (7534) (2015) 391-395.
10) M.A. Olayioye, R.M. Neve, H.A. Lane, N.E. Hynes, The ErbB signaling network: receptor heterodimerization in development and cancer, The EMBO journal 19 (13) (2000) 3159-3167.
11) M.L. de Castro Barbosa, L.M. Lima, R. Tesch, C.M.R. Sant'Anna, F. Totzke, M.H. Kubbutat, C. Schächtele, S.A. Laufer, E.J. Barreiro, Novel 2-chloro-4-anilino-quinazoline derivatives as EGFR and VEGFR-2 dual inhibitors, Eur. J. Med. Chem. 71 (2014) 1-14.
12) Y. Chen, J. Wu, A. Wang, Z. Qi, T. Jiang, C. Chen, F. Zou, C. Hu, W. Wang, H. Wu, Discovery of N-(5-((5-chloro-4-((2-(isopropylsulfonyl) phenyl) amino) pyrimidin-2-yl) amino)-4-methoxy-2-(4-methyl-1, 4-diazepan-1-yl) phenyl) acrylamide (CHMFL-ALK/EGFR-050) as a potent ALK/EGFR dual kinase inhibitor capable of overcoming a variety of ALK/EGFR associated drug resistant mutants in NSCLC, Eur. J. Med. Chem. 139 (2017) 674-697.
13) Y.A. Elshaier, M.A. Shaaban, M.K.A. El Hamid, M.H. Abdelrahman, M.A. Abou-Salim, S.M. Elgazwi, F. Halaweish, Design and synthesis of pyrazolo [3, 4-d] pyrimidines: Nitric oxide releasing compounds targeting hepatocellular carcinoma, Biorg. Med. Chem. 25 (12) (2017) 2956-2970.
14) H.-Q. Zhang, F.-H. Gong, J.-Q. Ye, C. Zhang, X.-H. Yue, C.-G. Li, Y.-G. Xu, L.-P. Sun, Design and discovery of 4-anilinoquinazoline-urea derivatives as dual TK inhibitors of EGFR and VEGFR-2, Eur. J. Med. Chem. 125 (2017) 245-254.

15) Z. Song, S. Huang, H. Yu, Y. Jiang, C. Wang, Q. Meng, X. Shu, H. Sun, K. Liu, Y. Li, Synthesis and biological evaluation of morpholine-substituted diphenylpyrimidine derivatives (Mor-DPPYs) as potent EGFR T790M inhibitors with improved activity toward the gefitinib-resistant non-small cell lung cancers (NSCLC), Eur. J. Med. Chem. 133 (2017) 329-339.

16) Y. Zhang, L. Chen, H. Xu, X. Li, L. Zhao, W. Wang, B. Li, X. Zhang, 6, 7-Dimorpholinoalkoxy quinazoline derivatives as potent EGFR inhibitors with enhanced antiproliferative activities against tumor cells, Eur. J. Med. Chem. 147 (2018) 77-89.

17) P. Bonomi, Erlotinib: a new therapeutic approach for non-small cell lung cancer, Expert Opin. Investig. Drugs 12 (8) (2003) 1395-1401.

18) J.F. Vansteenkiste, Gefitinib (Iressa®): a novel treatment for non-small cell lung cancer, Expert Rev. Anticancer Ther. 4 (1) (2004) 5-17.

19) M. Tiseo, M. Loprevite, A. Ardizzoni, Epidermal growth factor receptor inhibitors: a new prospective in the treatment of lung cancer, Curr. Med. Chem. Anti-Canc. Agents 4 (2) (2004) 139-148.

20) S. Kobayashi, T.J. Boggon, T. Dayaram, P.A. Jänne, O. Kocher, M. Meyerson, B.E. Johnson, M.J. Eck, D.G. Tenen, B. Halmos, EGFR mutation and resistance of non–small-cell lung cancer to gefitinib, N. Engl. J. Med. 2005 (352) (2005) 786-792.

21) E.L. Kwak, R. Sordella, D.W. Bell, N. Godin-Heymann, R.A. Okimoto, B.W. Brannigan, P.L. Harris, D.R. Driscoll, P. Fidias, T.J. Lynch, Irreversible inhibitors of the EGF receptor may circumvent acquired resistance to gefitinib, Proc. Nati. Acad. Sci. USA. 102 (21) (2005) 7665-7670.

22) S.-H.I. Ou, Second-generation irreversible epidermal growth factor receptor (EGFR) tyrosine kinase inhibitors (TKIs): a better mousetrap? A review of the clinical evidence, Crit. Rev. Oncol. Hematol. 83 (3) (2012) 407-421.

23) J. McIntyre, J. Castaner, P. Leeson, Canertinib dihydrochloride, Drugs Future 30 (2005) 771-779.

24) [24] L.V. Sequist, B. Besse, T.J. Lynch, V.A. Miller, K.K. Wong, B. Gitlitz, K. Eaton, C. Zacharchuk, A. Freyman, C. Powell, Neratinib, an irreversible pan-

ErbB receptor tyrosine kinase inhibitor: results of a phase II trial in patients with advanced non–small-cell lung cancer, J. Clin. Oncol. 28 (18) (2010) 3076-3083.

25) Y. Kim, J. Ko, Z. Cui, A. Abolhoda, J.S. Ahn, S.-H. Ou, M.-J. Ahn, K. Park, The EGFR T790M mutation in acquired resistance to an irreversible second-generation EGFR inhibitor, Mol. Cancer Ther. 11 (3) (2012) 784-791.

26) A.O. Walter, R.T.T. Sjin, H.J. Haringsma, K. Ohashi, J. Sun, K. Lee, A. Dubrovskiy, M. Labenski, Z. Zhu, Z. Wang, Discovery of a mutant-selective covalent inhibitor of EGFR that overcomes T790M-mediated resistance in NSCLC, Cancer discov. 3 (12) (2013) 1404-1415.

27) X. Xu, Parallel phase 1 clinical trials in the US and in China: accelerating the test of avitinib in lung cancer as a novel inhibitor selectively targeting mutated EGFR and overcoming T790M-induced resistance, Chin. j. cancer 34 (3) (2015) 27.

28) A. Yver, Osimertinib (AZD9291)—a science-driven, collaborative approach to rapid drug design and development, Ann. Oncol. 27 (6) (2016) 1165-1170.

29) S. Schenone, M. Radi, F. Musumeci, C. Brullo, M. Botta, Biologically driven synthesis of pyrazolo [3, 4-d] pyrimidines as protein kinase inhibitors: an old scaffold as a new tool for medicinal chemistry and chemical biology studies, Chem. Rev. 114 (14) (2014) 7189-7238.

30) S.M. El-Moghazy, R.F. George, E.E.A. Osman, A.A. Elbatrawy, M. Kissova, A. Colombo, E. Crespan, G. Maga, Novel pyrazolo [3, 4-d] pyrimidines as dual Src-Abl inhibitors active against mutant form of Abl and the leukemia K-562 cell line, Eur. J. Med. Chem. 123 (2016) 1-13.

31) C. Fraser, J.C. Dawson, R. Dowling, D.R. Houston, J.T. Weiss, A.F. Munro, M. Muir, L. Harrington, S.P. Webster, M.C. Frame, Rapid discovery and structure–activity relationships of pyrazolopyrimidines that potently suppress breast cancer cell growth via SRC kinase inhibition with exceptional selectivity over ABL kinase, J. Med. Chem. 59(10) (2016) 4697-4710.

32) S.N. Milik, D.S. Lasheen, R.A. Serya, K.A. Abouzid, How to train your inhibitor: Design strategies to overcome resistance to Epidermal Growth Factor Receptor inhibitors, Eur. J. Med. Chem. 142 (2017) 131-151.

33) P. Traxler, G. Bold, J. Frei, M. Lang, N. Lydon, H. Mett, E. Buchdunger, T. Meyer, M. Mueller, P. Furet, Use of a pharmacophore model for the design of EGF-R tyrosine kinase inhibitors: 4-(phenylamino) pyrazolo [3, 4-d] pyrimidines, J. Med. Chem. 40(22) (1997) 3601-3616.

34) R. Ducray, P. Ballard, B.C. Barlaam, M.D. Hickinson, J.G. Kettle, D.J. Ogilvie, C.B. Trigwell, Novel 3-alkoxy-1H-pyrazolo [3, 4-d] pyrimidines as EGFR and erbB2 receptor tyrosine kinase inhibitors, Biorg. Med. Chem. Lett. 18 (3) (2008) 959-962.

35) W.M. Eldehna, M.F. Abo-Ashour, A. Nocentini, P. Gratteri, I.H. Eissa, M. Fares, O.E. Ismael, H.A. Ghabbour, M.M. Elaasser, H.A. Abdel-Aziz, Novel 4/3-((4-oxo-5-(2-oxoindolin-3-ylidene) thiazolidin-2-ylidene) amino) benzenesulfonamides: Synthesis, carbonic anhydrase inhibitory activity, anticancer activity and molecular modelling studies, Eur. J. Med. Chem. 139 (2017) 250-262.

36) [I.H. Eissa, A.M. El-Naggar, M.A. El-Hashash, Design, synthesis, molecular modeling and biological evaluation of novel 1H-pyrazolo [3, 4-b] pyridine derivatives as potential anticancer agents, Bioorg. Chem. 67 (2016) 43-56.

37) [37] I. Eissa, A. El-Naggar, N. El-Sattar, A. Youssef, Design and discovery of novel quinoxaline derivatives as dual DNA intercalators and topoisomerase II inhibitors, Anti-cancer agents in medicinal chemistry 18 (2018) 195-209.

38) A.M. El-Naggar, M.M. Abou-El-Regal, S.A. El-Metwally, F.F. Sherbiny, I.H. Eissa, Synthesis, characterization and molecular docking studies of thiouracil derivatives as potent thymidylate synthase inhibitors and potential anticancer agents, Molecular diversity 21(4) (2017) 967-983.

39) M.K. Ibrahim, M.S. Taghour, A.M. Metwaly, A. Belal, A.B.M. Mehany, M.A. Elhendawy, M.M. Radwan, A.M. Yassin, N.M. El-Deeb, E.E. Hafez, M.A. ElSohly, I.H. Eissa, Design, synthesis, molecular modeling and anti-proliferative evaluation of novel quinoxaline derivatives as potential DNA intercalators and topoisomerase II inhibitors, Eur. J. Med. Chem. 155 (2018) 117-134.

40) V. Gandin, A. Ferrarese, M. Dalla Via, C. Marzano, A. Chilin, G. Marzaro, Targeting kinases with anilinopyrimidines: discovery of N-phenyl-N'-[4-

(pyrimidin-4-ylamino) phenyl] urea derivatives as selective inhibitors of class III receptor tyrosine kinase subfamily, Sci. Rep. 5 (2015) 16750.

41) P. Traxler, P. Furet, Strategies toward the design of novel and selective protein tyrosine kinase inhibitors, Pharmacol. Ther. 82 (2-3) (1999) 195-206.

42) J. Zhang, P.L. Yang, N.S. Gray, Targeting cancer with small molecule kinase inhibitors, Nat. Rev. Cancer 9 (1) (2009) 28-39.

43) V.K. Sharma, P.P. Nandekar, A. Sangamwar, H. Pérez-Sánchez, S.M. Agarwal, Structure guided design and binding analysis of EGFR inhibiting analogues of erlotinib and AEE788 using ensemble docking, molecular dynamics and MM-GBSA, RSC Adv. 6 (70) (2016) 65725-65735.

44) S. Mowafy, A. Galanis, Z.M. Doctor, R.M. Paranal, D.S. Lasheen, N.A. Farag, P.A. Jänne, K.A. Abouzid, Toward discovery of mutant EGFR inhibitors; Design, synthesis and in vitro biological evaluation of potent 4-arylamino-6-ureido and thioureido-quinazoline derivatives, Biorg. Med. Chem. 24 (16) (2016) 3501-3512.

45) Z. Zhao, H. Wu, L. Wang, Y. Liu, S. Knapp, Q. Liu, N.S. Gray, Exploration of type II binding mode: a privileged approach for kinase inhibitor focused drug discovery?, ACS Chem. Biol. 9 (6) (2014) 1230-1241.

46) P. Furet, G. Caravatti, N. Lydon, J.P. Priestle, J.M. Sowadski, U. Trinks, P. Traxler, Modelling study of protein kinase inhibitors: binding mode of staurosporine and origin of the selectivity of CGP 52411, J. Comput. Aided Mol. Des. 9 (6) (1995) 465-472.

47) Y. Liu, N.S. Gray, Rational design of inhibitors that bind to inactive kinase conformations, Nat. Chem. Biol. 2 (7) (2006) 358-364.

48) P. Traxler, P. Furet, Strategies toward the design of novel and selective protein tyrosine kinase inhibitors, Pharmacol. Ther. 82 (2) (1999) 195-206.

49) R. Li, H. Tang, H. Fu, H. Ren, X. Wang, C. Wu, C. Wu, F. Shi, Arynes double bond insertion/nucleophilic addition with vinylogous amides and carbodiimides, J. Org. Chem. 79 (3) (2014) 1344-1355.

50) H.-Y. He, J.-N. Zhao, R. Jia, Y.-L. Zhao, S.-Y. Yang, L.-T. Yu, L. Yang, Novel pyrazolo [3, 4-d] pyrimidine derivatives as potential antitumor agents: exploratory

synthesis, preliminary structure-activity relationships, and in vitro biological evaluation, Molecules 16 (12) (2011) 10685-10694.

51) A. Miyashita, C. Iijima, T. Higashino, Studies on pyrazolo [3, 4-d] pyrimidine derivatives. XVIII, Facile preparation of 1H-pyrazolo [3, 4-d] pyrimidin-4 [5H]-ones, Heterocycles 31 (7) (1990) 1309-1314.

52) A. Miyashita, Y. Suzuki, K.-i. Iwamoto, T. Higashino, Catalytic action of azolium salts. IX. Synthesis of 6-aroyl-9H-purines and their analogues by nucleophilic aroylation catalyzed by imidazolium or benzimidazolium salt, Chem. Pharm. Bull. 46 (3) (1998) 390-399.

53) M.-K. Ibrahim, A.A. Abd-Elrahman, R.R. Ayyad, K. El-Adl, A.M. Mansour, I.H. Eissa, Design and synthesis of some novel 2-(3-methyl-2-oxoquinoxalin-1 (2H)-yl)-N-(4-(substituted) phenyl) acetamide derivatives for biological evaluation as anticonvulsant agents, Bull Faculty Pharm Cairo Univ. 51 (1) (2013) 101-111.

54) M.K. Ibrahim, I.H. Eissa, A.E. Abdallah, A.M. Metwaly, M. Radwan, M. ElSohly, Design, synthesis, molecular modeling and anti-hyperglycemic evaluation of novel quinoxaline derivatives as potential PPARγ and SUR agonists, Biorg. Med. Chem. 25 (4) (2017) 1496-1513.

55) M.K. Ibrahim, I.H. Eissa, M.S. Alesawy, A.M. Metwaly, M.M. Radwan, M.A. ElSohly, Design, synthesis, molecular modeling and anti-hyperglycemic evaluation of quinazolin-4 (3H)-one derivatives as potential PPARγ and SUR agonists, Biorg. Med. Chem. 25 (17) (2017) 4723-4744.

56) A.G.A. El-Helby, R.R. Ayyad, H.M. Sakr, A.S. Abdelrahim, K. El-Adl, F.S. Sherbiny, I.H. Eissa, M.M. Khalifa, Design, synthesis, molecular modeling and biological evaluation of novel 2, 3-dihydrophthalazine-1, 4-dione derivatives as potential anticonvulsant agents, J. Mol. Struct. 1130 (2017) 333-351.

57) A.-G.A. El-Helby, R.R. Ayyad, K. El-Adl, H. Sakr, A.A. Abd-Elrahman, I.H. Eissa, A. Elwan, Design, molecular docking and synthesis of some novel 4-acetyl-1-substituted-3, 4-dihydroquinoxalin-2 (1H)-one derivatives for anticonvulsant evaluation as AMPA-receptor antagonists, Med. Chem. Res. 25 (12) (2016) 3030-3046.

58) K.M. El-Gamal, A.M. El-Morsy, A.M. Saad, I.H. Eissa, M. Alswah, Synthesis, docking, QSAR, ADMET and antimicrobial evaluation of new quinoline-3-carbonitrile derivatives as potential DNA-gyrase inhibitors, J. Mol. Struct. 1166 (2018) 15-33.

59) Y. Jia, C.M. Quinn, A.I. Gagnon, R. Talanian, Homogeneous time-resolved fluorescence and its applications for kinase assays in drug discovery, Anal. Biochem. 356 (2) (2006) 273-281.

60) J. van Meerloo, G.J. Kaspers, J. Cloos, Cell sensitivity assays: the MTT assay, Cancer cell culture, 2nd edition, (2011) 237-245.

61) P. Li, Q. Zhang, A. Torossian, Z.-b. Li, W.-c. Xu, B. Lu, S. Fu, Simultaneous inhibition of EGFR and PI3K enhances radiosensitivity in human breast cancer, Int. J. Radiat. Oncol. Biol. Phys. 83 (3) (2012) 391-397.

62) A. Huether, M. Höpfner, V. Baradari, D. Schuppan, H. Scherübl, EGFR blockade by cetuximab alone or as combination therapy for growth control of hepatocellular cancer, Biochem. Pharmacol. 70 (11) (2005) 1568-1578.

63) S. Van Schaeybroeck, J. Kyula, D.M. Kelly, A. Karaiskou-McCaul, S.A. Stokesberry, E. Van Cutsem, D.B. Longley, P.G. Johnston, Chemotherapy-induced epidermal growth factor receptor activation determines response to combined gefitinib/chemotherapy treatment in non–small cell lung cancer cells, Mol. Cancer Ther. 5 (5) (2006) 1154-1165.

64) B.M. Ku, Y.-H. Bae, J. Koh, J.-M. Sun, S.-h. Lee, J.S. Ahn, K. Park, M.-J. Ahn, AZD9291 overcomes T790 M-mediated resistance through degradation of EGFRL858R/T790M in non-small cell lung cancer cells, Invest. New Drugs 34 (4) (2016) 407-415.

65) Y. Murakami, K. Sonoda, H. Abe, K. Watari, D. Kusakabe, K. Azuma, A. Kawahara, J. Akiba, C. Oneyama, J.A. Pachter, The activation of SRC family kinases and focal adhesion kinase with the loss of the amplified, mutated EGFR gene contributes to the resistance to afatinib, erlotinib and osimertinib in human lung cancer cells, Oncotarget 8 (41) (2017) 70736.

66) I. Vermes, C. Haanen, H. Steffens-Nakken, C. Reutellingsperger, A novel assay for apoptosis flow cytometric detection of phosphatidylserine expression on early

apoptotic cells using fluorescein labelled annexin V, J. Immunol. Methods 184 (1) (1995) 39-51.

67) A. Huether, M. Höpfner, A.P. Sutter, D. Schuppan, H. Scherübl, Erlotinib induces cell cycle arrest and apoptosis in hepatocellular cancer cells and enhances chemosensitivity towards cytostatics, J. Hepatol. 43 (4) (2005) 661-669.

68) J.H. Park, Y. Liu, M.A. Lemmon, R. Radhakrishnan, Erlotinib binds both inactive and active conformations of the EGFR tyrosine kinase domain, Biochem. J 448 (3) (2012) 417-423.

69) S. Sogabe, Y. Kawakita, S. Igaki, H. Iwata, H. Miki, D.R. Cary, T. Takagi, S. Takagi, Y. Ohta, T. Ishikawa, Structure-based approach for the discovery of pyrrolo [3, 2-d] pyrimidine-based EGFR T790M/L858R mutant inhibitors, ACS Med. Chem. Lett. 4 (2) (2012) 201-205.

70) Chemical Computing Group, Molecular Operating Environment (MOE), http://www.chemcomp.com/ (Accessed in May 2017).

Highlights

- Thirty compounds of novel 1*H*-pyrazolo[3,4-*d*]pyrimidine derivatives were designed and synthesized.
- *In vitro* anti $EGFR^{WT}$ and $EGFR^{T790M}$ activity were evaluated.
- Anti-proliferative activity were tested against five cancel cell lines.
- Molecular docking studies were carried out against $EGFR^{WT}$ and $EGFR^{T790M}$.

Graphical abstarct: